The Ets Transcription Factor EHF as a Regulator of Cornea Epithelial Cell Identity*[S]

Denise N. Stephens[‡], Rachel Herndon Klein[‡§], Michael L. Salmans[‡§], William Gordon[‡], Hsiang Ho[¶], and Bogi Andersen[‡§¶1]

From the Departments of [‡]Biological Chemistry and [¶]Medicine and the [§]Institute for Genomics and Bioinformatics, University of California, Irvine, California 92697

Background: Cornea development requires precise, coordinated gene expression; few regulators have been characterized.
Results: Ets factor EHF collaborates with Kruppel-like factors to activate cornea epithelial genes while repressing non-epithelial genes.
Conclusion: EHF, in collaboration with other transcription factors, promotes cornea epithelial identity.
Significance: We generated a comprehensive data set on cornea gene expression over the lifetime of the mouse, identifying novel regulators of cornea epithelial identity.

The cornea is the clear, outermost portion of the eye composed of three layers: an epithelium that provides a protective barrier while allowing transmission of light into the eye, a collagen-rich stroma, and an endothelium monolayer. How cornea development and aging is controlled is poorly understood. Here we characterize the mouse cornea transcriptome from early embryogenesis through aging and compare it with transcriptomes of other epithelial tissues, identifying cornea-enriched genes, pathways, and transcriptional regulators. Additionally, we profiled cornea epithelium and stroma, defining genes enriched in these layers. Over 10,000 genes are differentially regulated in the mouse cornea across the time course, showing dynamic expression during development and modest expression changes in fewer genes during aging. A striking transition time point for gene expression between postnatal days 14 and 28 corresponds with completion of cornea development at the transcriptional level. Clustering classifies co-expressed, and potentially co-regulated, genes into biologically informative categories, including groups that exhibit epithelial or stromal enriched expression. Based on these findings, and through loss of function studies and ChIP-seq, we show that the Ets transcription factor EHF promotes cornea epithelial fate through complementary gene activating and repressing activities. Furthermore, we identify potential interactions between EHF, KLF4, and KLF5 in promoting cornea epithelial differentiation. These data provide insights into the mechanisms underlying epithelial development and aging, identifying EHF as a regulator of cornea epithelial identity and pointing to interactions between Ets and KLF factors in promoting epithelial fate. Furthermore, this comprehensive gene expression data set for the cornea is a powerful tool for discovery of novel cornea regulators and pathways.

The cornea is the transparent tissue at the front of the eye, responsible for transmission and focusing of light through the iris while also protecting the eye from infections and other external damage. The cornea consists of three cellular layers: the outermost non-keratinized, stratified epithelium; the intermediate stroma, which in mammals comprises up to 90% of the cornea's thickness; and the innermost single layered endothelium (1). In the mouse, cornea development (Fig. 1A) begins around embryonic day 12. The epithelium differentiates from the surface ectoderm with KRT14 (keratin 14) expression marking the transition from ectoderm to cornea epithelium. Around the same time, mesenchymal cells from the neural crest migrate into the space between the ectoderm and the lens (2), ultimately differentiating into stromal fibroblasts (keratocytes) and the endothelium (3). The stroma and endothelium undergo organization during the late embryonic and early postnatal period; keratocytes differentiate and secrete extracellular matrix proteins, including collagen, and the endothelium proliferates, forming a monolayer across the posterior cornea. Meanwhile, the epithelium undergoes progressive stratification and differentiation in late embryogenesis and during the early postnatal period. By 2 weeks of age, the epithelium reaches nearly full thickness, and terminal differentiation markers, such as KRT12 and GJA1(Cx43), are visible. The stroma has become thicker and largely acellular, and the endothelial cells cease proliferation, having formed a barrier to maintain the fluid balance in the stroma (4).

In cornea aging, morphological changes are subtle (Fig. 1A) (5). Expression of cellular adhesion molecules in the epithelium decreases, and the epithelium loses repair capacity, becoming more vulnerable to infections. Collagen synthesis in the stroma is reduced, and the cornea, one of the most highly innervated

tissues in the body, loses sensitivity. Endothelial cell density also decreases (6). Although the morphology of the mouse cornea during development and in the adult has been well characterized (2, 7, 8), there have only been a few studies characterizing the global gene expression of the normal cornea (1, 9–11), none of them profiling gene expression over stages of development and adulthood.

Here we have created a comprehensive gene expression profile of whole mouse cornea at key points throughout cornea development and every 6 months thereafter, from age E14.5[2] to 2 years postnatally. This data set will be useful for the discovery of new genes, gene groups, transcriptional regulators, and biologically important pathways in the cornea and will also assist in the characterization of transgenic mouse models and human cornea diseases. Using these data, we identified the Ets factor EHF (Ets homologous factor) as a potential regulator of cornea epithelial cell differentiation, and through a combination of ChIP-seq and RNAi, we demonstrate for the first time that EHF promotes cornea epithelial cell identity.

EXPERIMENTAL PROCEDURES

Isolation of Total RNA and Preparation for Whole Genome Expression Arrays—Whole corneas were dissected from wild type CB6 mouse eye globes. Cornea epithelium was isolated from P28 mice by digestion in 50% EMEM, dispase II with 50 mM sorbitol and 10 μl/ml β-mercaptoethanol for 2 h at 37 °C (modified from Ref. 12). The corneal stroma was isolated from P7 mice by embedding whole eye globes in OCT, cryosectioning at 10 μm, and microdissecting out the stroma. Total RNA from cornea and other tissues was isolated as described previously (13). Sample purity was validated by quantitative PCR expression of tissue-specific markers and the absence of markers for adjacent tissues. Cornea samples were prepared for microarray with the NuGEN Ovation RNA Amplification System V2 and NuGEN FL-Ovation cDNA Biotin Module V2 (NuGEN Technologies, San Carlos CA). All other samples were prepared with the Ambion WT expression kit (Invitrogen). Whole genome expression was assessed with Affymetrix Mouse Gene 1.0 ST arrays in triplicate (E14.5–P60 cornea; lung, trachea) or duplicate (P180 to 2-year cornea; separated epithelium and stroma) and Mouse Genome 430 arrays in triplicate (esophagus, small intestine, stomach, and skin). Microarray data for bladder and E18.5 skin was published previously (13).

Microarray Data Analysis—Array data were quantified with Expression Console version 1.1 software (Affymetrix, Inc.) using the PLIER Algorithm default values. Expression values were then filtered as present/absent at expression 150. Only known coding transcripts (24,582) representing 21,676 genes (referred to here as the transcriptome) were included in the analysis. MultiExperiment Viewer software (14, 15) was used to perform analysis of variance, principal component analysis (PCA), gene distance matrix, hierarchical clustering, and k-means analyses. Probe sets were called differentially expressed if they had a p value of <0.01 and a 2-fold expression

change over the developmental time course. The Cyber-T web server (16, 17) was utilized to compare P28–P60 and 2-year whole cornea samples; genes passing a p value of <0.05 and a change in expression greater than 1.3-fold were clustered with hierarchical clustering. The Cyber-T method was also used to determine differential expression between epithelium and stroma; epithelium-enriched, stroma-enriched, or both (expressed in both samples) probe sets were determined by a -fold expression cut-off using known markers in each tissue. We used AmiGO (18) to compile a list of mouse transcriptional regulators, including DNA-binding transcription factors, chromatin modifiers, and transcription co-factors. For comparison across epithelial tissues, each array was log$_2$-transformed and mean-centered with the S.D. set to 1. Only common probe sets from Affymetrix Mouse Gene 430 and Affymetrix MoGene 1.0 ST arrays were used for downstream analyses. For the gene distance matrix, gene chip biases were removed using distance-weighted discrimination (19). For identification of genes unique to the cornea, sample replicates were averaged, and -fold changes were calculated by comparing each tissue at E18.5 with the cornea P28 sample. Genes with -fold change ±2.0 in all other tissues were selected for hierarchical clustering and k-means clustering ($k = 7$). Clustering and heat maps were generated using the pheatmap package in R (available from the R Project for Statistical Computing Web site). For comparing aging gene expression changes across tissues, we obtained data from previously published expression data sets and from GEO (Gene Expression Omnibus) (20–36). Gene ontology was performed using DAVID (37, 38).

ChIP-PCR and ChIP Sequencing—ChIP assays were performed as described previously (13, 39), using IgG (Sigma; for ChIP-PCR only) or EHF antibody (Santa Cruz Biotechnology, Inc.; for ChIP-PCR and ChIP-seq). Sequencing libraries were generated for the EHF ChIP and input samples using the Illumina Tru-Seq kit, according to the Illumina protocol for ChIP-seq library preparation with some modification; after adaptor ligation, 14 cycles of PCR amplification were performed prior to size selection of the library (40). Clustering and 50-cycle single end sequencing were performed on the Illumina Hi-Seq 2000 genome analyzer. Reads were aligned to the mouse mm9 genome using Bowtie (version 0.12.7) (41), with only uniquely aligning reads retained; in total, 6.5 million mapped reads were obtained. MACS (version 1.4.2) (42) was used to call peaks, with the input sample used as the control. Galaxy was used to align peaks to gene regions and compare ChIP-seq and siRNA data (43–45). MEME and Cistrome were used for motif analysis (46, 47).

Whole Genome Expression Arrays for Primary Human Cornea Epithelial Cells and siRNA Experiments—Primary human cornea epithelial cells from CELLnTEC Inc. were grown in CnT-20 medium as directed by the manufacturer. Cells were trypsinized and plated, 100,000 cells/well, in a 12-well dish containing 1 μl of Lipofectamine RNAiMAX and either 30 nM *EHF* siRNA or scrambled siRNA. The *EHF* siRNA was pooled from three individual siRNAs targeting *EHF* (Ambion, ID s25397, s25398, s25399) in the same concentration. *EHF* mRNA knockdown was verified by quantitative PCR, and reduction in EHF protein level was demonstrated in immortalized human cornea epithelial cells by Western blot. Total RNA was extracted from

---

[2] The abbreviations used are: E*n*, embryonic day *n*; P*n*, postnatal day *n*; GO, gene ontology; PCA, principal component analysis; ChIP-seq, ChIP sequencing.
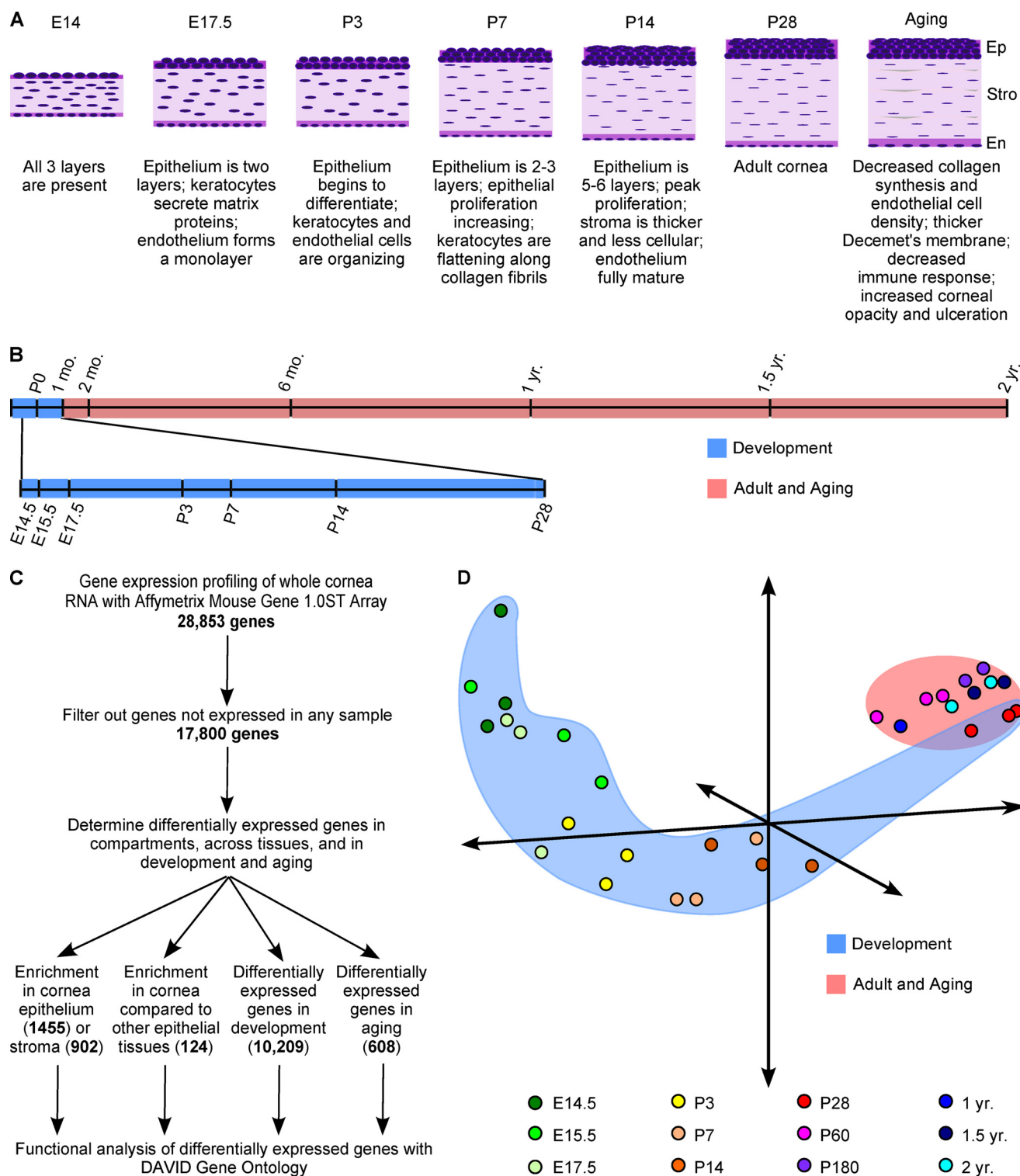
FIGURE 1. **Cornea gene expression over the lifetime of the mouse.** *A*, schematic representation of the main features of cornea development and aging in the mouse. *B*, time line depicting the ages of mouse cornea samples used in whole genome expression time course analysis. *C*, work flow of microarray data analysis. Genes with an expression <150 in all samples were filtered out. *D*, principle component analysis of all samples used in the expression time course. *Axes* represent the two time points with greatest variation. Samples taken at P28 and later cluster together (*pink area*), whereas samples from earlier time points exhibit greater change (*blue area*). *Ep*, epithelium; *Stro*, stroma; *En*, endothelium.

the plated cells with the Purelink RNA miniprep kit (Ambion) 72 h after transfection. Samples were prepared for the array with the Ambion WT expression kit, and whole genome expression was assessed with Affymetrix Human Gene 1.0 ST arrays. The experiment was performed with three biological replicates. The Cyber-T method was used to determine statistically differentially expressed genes.

Data Access—GEO data sets referred to in this paper are as follows: GSE43155, expression profiling of wild type mouse cornea in development, adult, and aging; GSE43157, expression

TABLE 1

Expression of characteristic cornea genes correlates well with previous studies

Well characterized cornea-expressed genes were compared with mRNA expression data from the indicated publications. The cluster membership (see Fig. 3) is indicated for each gene.

Gene symbol	Cluster	Reference
Klf6	C22	Nakamura *et al.* (51)
Sp1	C25	Nakamura *et al.* (105)
Krt12	C1	Tanifuji-Terai *et al.* (52)
Kera	C5	Liu *et al.* (49)
Tkt	C13	Sax *et al.* (48)
Bgn	C7	Zhang *et al.* (42)
Dcn	C20	Zhang *et al.* (42)
Ese1	C12	Yoshida *et al.* (50)
Krt14	C18	Tanifuji-Terai *et al.* (52)
Hes1	C23	Nakamura *et al.* (54)
Emp2	C13	Wu *et al.* (9)
Sema4a	C23	Wu *et al.* (9)
Npy	C18	Wu *et al.* (9)
Aldh3a1	C1	Davis *et al.* (53)

data from siRNA knockdown of *EHF* in primary human cornea epithelial cells; GSE43381, expression profiling across mouse epithelial tissues; and GSE44741, genome-wide binding of EHF in mouse cornea epithelium.

RESULTS

A Transcriptome Profile over the Lifetime of the Cornea Identifies a Development-Adulthood Transition Point—To identify new regulators of cornea development, homeostasis, and aging, we defined the global gene expression profile of the whole cornea over the lifetime of the mouse, beginning at embryonic day 14.5 and continuing through adulthood to age 2 years (Fig. 1, *A* and *B*). Using gene expression microarrays, we found that 17,800 genes (19,783 probe sets; 75% of the mouse transcriptome) are expressed in at least one time point of the time course (Fig. 1*C*). Expression of selective genes corresponded well with data from previous more focused studies (2–9, 42, 48–54), indicating the validity of our data set (Table 1). Utilizing PCA, the samples fell into two distinct groups in terms of overall similarity: P28 to 2 year (adult/aging samples), which are highly similar to one another, and the developmental samples, which show drastic changes over time (Fig. 1*D*). Consistent with the highly dynamic gene expression during cornea development, the greatest number of genes change expression during two of the developmental transition points, E14.5–E15.5 and P14–P28 (Fig. 2*A*). Because the P28 samples cluster tightly with the adult samples, these data suggest that by gene expression criteria, cornea development is essentially completed by P28.

To search for gene expression patterns matching the phases of development and adulthood as defined by PCA, we identified genes showing greater than 2-fold average change in expression between the developmental (E14.5–P14) and adult (P28 to 2 year) time points. Remarkably, 1106 genes feature a striking expression switch at the P14–P28 development-adulthood transition point (Fig. 2*B*). Gene ontology (GO) analysis of these genes identified overrepresentation of genes associated with specific functions in the two phases, indicating the activity of distinct biological processes during cornea development and adult homeostasis. During development, the biological terms *cell adhesion*, *extracellular matrix organization*, *myofibril assembly*, and *cell motion* most likely represent active migration

of cornea keratocytes and keratinocytes characteristic for morphogenesis of the cornea (Fig. 2*C*). During adulthood, the biological terms *lipid biosynthetic process*, *oxidation reduction*, and *response to abiotic stimulus* most likely represent the cornea's role as a barrier to environmental exposure, which becomes more important as the cornea fully differentiates (Fig. 2*D*). Together, these data point to an important gene expression transition point between P14 and P28 that reflects distinct functions of the developing and adult cornea.

Distinct Spatio-temporal Gene Expression Profiles Underlie Cornea Development—The PCA analysis (Fig. 1*D*), and the identification of a transcriptional switch at the development-adult transition point (Fig. 2*B*), suggested that gene expression could be analyzed separately for the development and adulthood phases, using P28 as the end point for development and the starting point for adulthood. We first investigated gene expression patterns during development from E14.5 to P28 by analysis of variance, identifying 10,209 genes (12,000 probe sets; 43% of the mouse transcriptome) as significantly differentially regulated over the developmental time course. *k*-Means clustering grouped the developmentally regulated genes by their temporal expression pattern into 40 distinct clusters (Fig. 3 and supplemental Table S1). To facilitate classification of the temporal gene expression clusters vis á vis epithelial and stromal expression, we evaluated the ratio of probe set expression in isolated adult cornea epithelium and stroma (Fig. 4*A*). By setting cut-offs based on the -fold enrichment of numerous known epithelial and stromal genes, we generated a list of epithelial (1832 probe sets, 1455 genes) and stromal (1147 probe sets, 902 genes) enriched genes, representing 6 and 4% of the mouse transcriptome, respectively. We then overlapped the lists of "epithelial" and "stromal" genes with the developmental clusters, discovering that a number of clusters contained a significant overrepresentation of epithelial or stromal enriched genes, whereas other clusters were composed of genes expressed relatively equally in both cell layers (Fig. 4*B*).

We observed that the shapes of the temporal expression patterns in some clusters were similar and that they differed mostly in the magnitude of gene expression change (Fig. 3); many of these clusters also contained similar GO terms (Table 2). Using these temporal pattern similarities, and considering membership of known marker genes as well as the representation of epithelium- and stroma-enriched genes, we combined 31 of the 40 *k*-means clusters into 10 superclusters (Fig. 5). Grouping the clusters in this manner resulted in three "epithelial" (*A*, *C*, and *G*) and four "stromal" (*B*, *E*, *F*, and *H*) superclusters. Of the remaining three superclusters, one supercluster (*D*) contains both epithelial and stromal genes, although it is slightly more stromal than epithelial in nature. The last two superclusters (*I* and *J*) are primarily composed of genes expressed in both epithelium and stroma, containing GO categories that represent housekeeping-type genes, and showing modest changes in expression.

Comparing the epithelial and stromal superclusters, the most striking difference is evident between P14 and P28 when expression in the epithelial clusters is increasing while expression in stromal clusters is decreasing (Fig. 5). This observation suggests that during this time period, increased expression of many epithelial
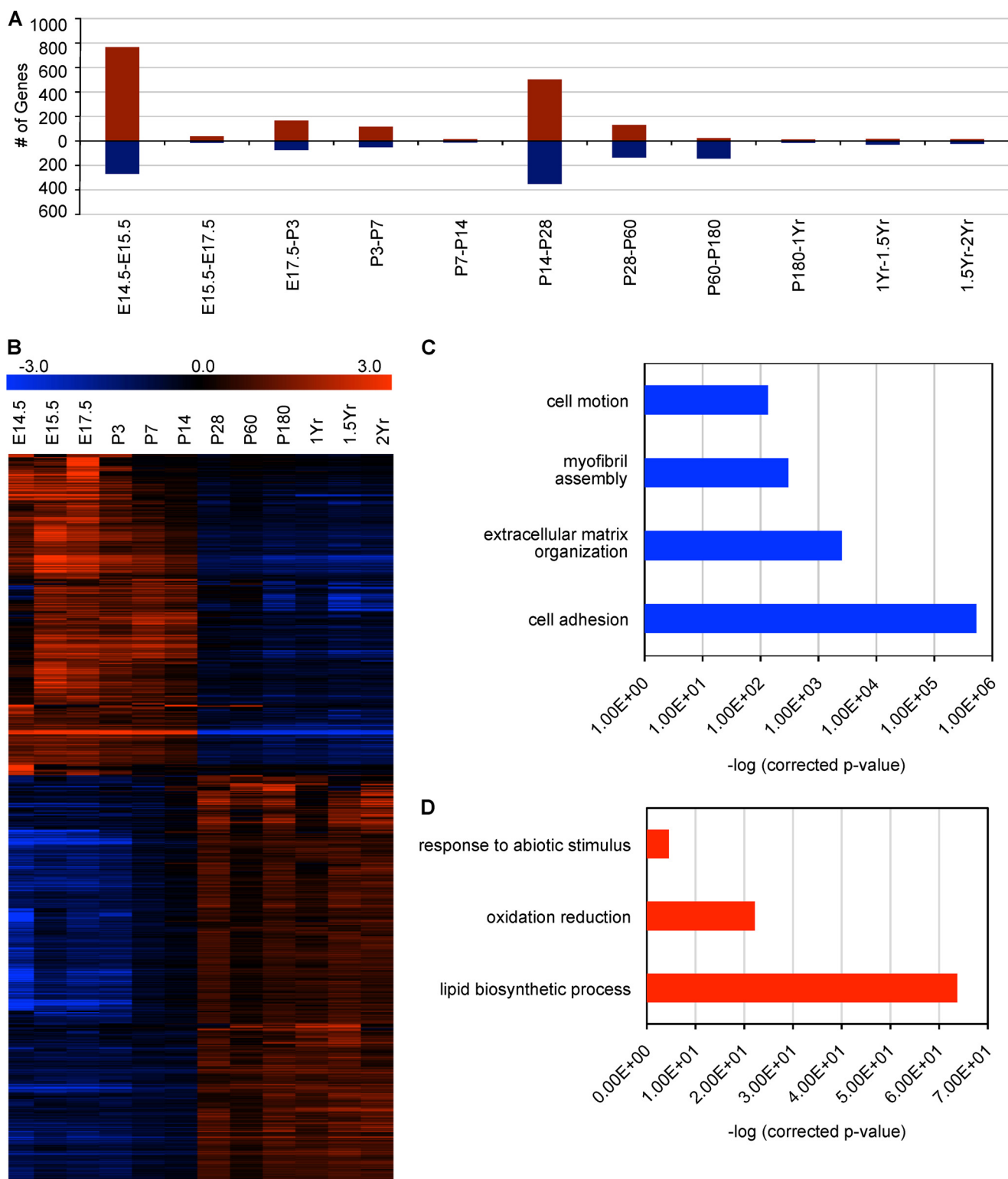
FIGURE 2. **Identification of a gene expression transition point between P14 and P28 points to the importance of distinct biological functions in cornea during development and adulthood.** *A*, number of differentially regulated genes ($p < 0.01$, >1.5-fold change) between the indicated time points. *Bars above* 0 (*red*) and *below* 0 (*blue*) represent the number of up- and down-regulated genes, respectively. The greatest number of genes exhibit expression change between E14.5 and E15.5, and between P14 and P28. *B*, a heat map showing expression of genes that are differentially regulated when all developmental time points are compared with all adult/aging time points. *C*, GO analysis of genes down-regulated between development and aging. *D*, GO analysis of genes up-regulated between development and aging.

genes is required for the formation of an effective epithelial barrier that protects the adult eye from injury and infection. Meanwhile, it is likely that the expression of many stromal components decreases during the same period to allow the cornea to develop a transparent state. Another difference between epithelial and stromal clusters is the respective up- and downward trend in gene
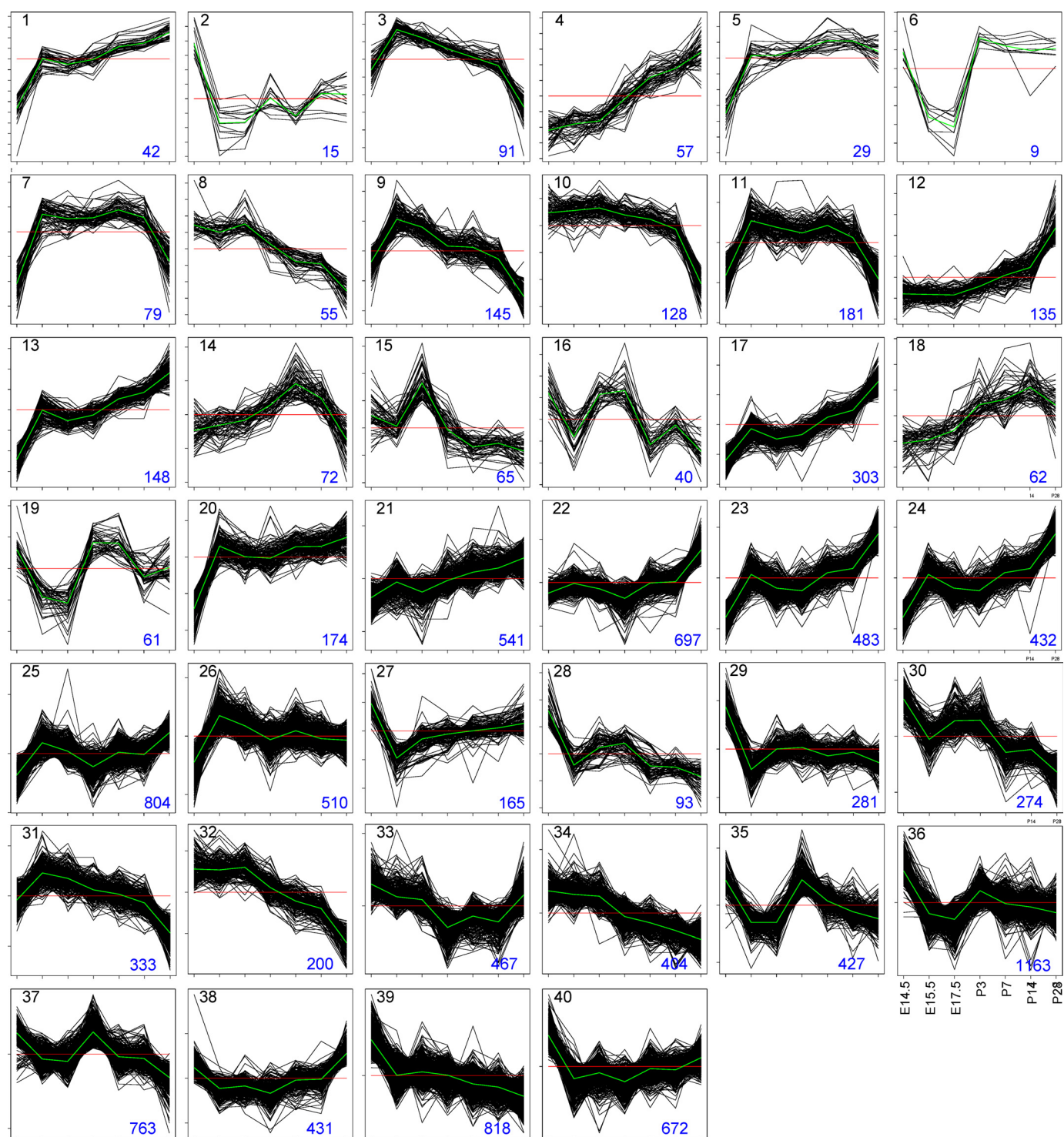
FIGURE 3. ***k*-Means clustering of developmental cornea expression data.** Differentially regulated genes were grouped into 40 temporal expression clusters. *x axis*, time point (*labels* shown on graph for cluster 36); *y axis*, $\log_2$ expression. Each *tick mark* represents 1-fold. *Red line*, 0. *Green line*, average expression value at each time point for all probe sets within the cluster. *Blue number* in the *lower right corner*, number of genes in each cluster.

expression over the whole time course. In particular, two of the three epithelial clusters (A and G) exhibit a robust up-regulation in gene expression between E14.5 and E15.5, corresponding to the formation of a two-layered epithelium.

Developmental Co-regulation of Cornea Genes Suggests New Transcriptional Regulators for Cornea—In addition to pointing to new biological functions through GO categories, the clusters

suggest linkage between transcriptional regulators (*TRs*) and target genes (Fig. 5). For example, cluster A contains the well characterized epithelial differentiation genes *Krt12*, *Aldh3a1*, and *Upk1b* (55–57) and known transcriptional regulators for epithelial differentiation, including *Klf4* and *Klf5* (58, 59). In fact, the KLF5 target genes *Dsp* and *Dsg1b* (59) are both found in this cluster. We overlapped the gene expression data for *Klf4*

FIGURE 4. **Evaluation of epithelial and stromal enrichment of genes expressed in the mouse cornea.** *A*, gene expression data for separated cornea epithelium and stroma samples at P28. Expression of each gene in the epithelium (*x axis*) was plotted against its expression in the stroma (*y axis*). The *lines* depict the cut-off for epithelium-enriched (*blue*) or stroma-enriched (*red*) genes. Enrichment of selected epithelial (*blue*) and stromal (*red*) markers are shown. *B*, epithelial and stromal enrich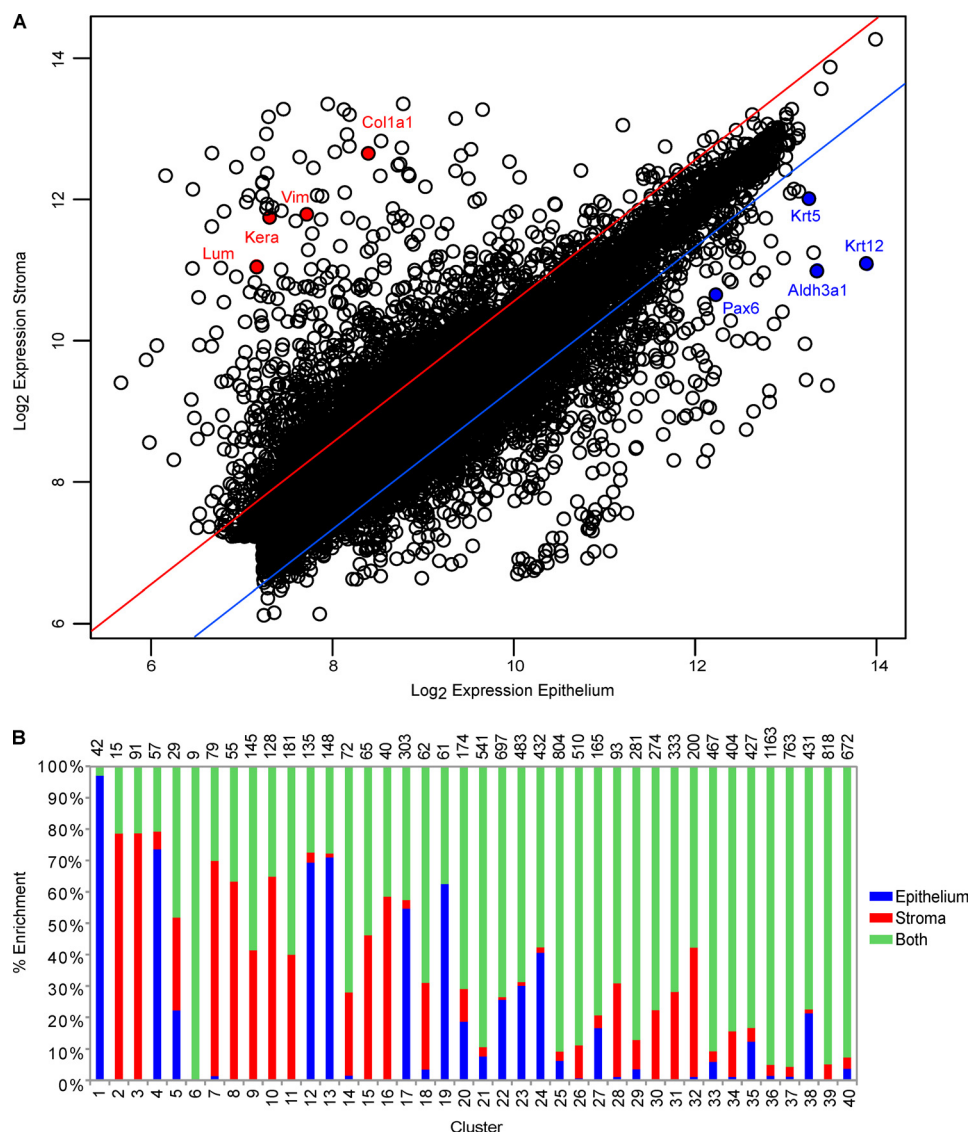ment of genes applied to the developmental *k*-means clusters. *Blue*, epithelial genes; *red*, stromal genes; *green*, genes expressed equally in both tissues. The number of probe sets in each cluster is shown at the *top* of its respective *column*.

and *Klf5* conditional knock-out corneas with the superclusters and observed differences in cluster membership between genes up-regulated and down-regulated after *Klf4* and *Klf5* deletion. For instance, genes that appear to be positively regulated by KLF4 and KLF5 (down-regulated after gene deletion) are enriched in epithelial-type superclusters like A and C. In contrast, genes that are up-regulated after deletion of these two factors tend to fall into stromal-type superclusters like B and E (Fig. 6).

Supercluster A also contains transcriptional regulators not previously known to have a function in the cornea epithelium, including the Ets factor EHF, a candidate new regulator for the cornea epithelial differentiation program. Cluster C contains Ets factor *Elf3* (*Ese1*), previously implicated in cornea epithelial differentiation (50), along with epithelial markers *Aqp5* and *Itga6* (60, 61). Interestingly, epithelial gene repressor *Zeb1* (62) and its uncharacterized family member *Zeb2* were located in

cluster E, a stromal cluster. Known stromal transcription factors *Pitx2* and *Twist2* (63, 64) were grouped in cluster B, which contained stromal markers *Fbln2*, *P4ha2* (65, 66), and genes enriched for positive regulation of cell-substrate adhesion. This cluster also contained *Twist1*, suggesting it as a potential regulator of stromal gene expression. We also examined where endothelial genes were located across the clusters and found them to be evenly distributed among the clusters (data not shown). We conclude that membership in the superclusters can be mined to develop new hypotheses about regulatory relationships in the cornea epithelium and stroma.

To identify genes uniquely expressed in the cornea compared with other epithelial tissues, we utilized previously published (13) and new microarray expression data from seven other mouse epithelial tissues, comparing these to gene expression during cornea development (Fig. 7). At the transcript level, the developing cornea most resembles E18.5 bladder and E14.5

TABLE 2

Characteristics of the developmental *k*-means clusters

Number of probe sets, selected known cornea-expressed genes (example genes), top significant GO categories, and proportion of epithelium- and stroma-enriched transcripts are listed. Transcriptional regulators are shown in boldface type. E, epithelium-enriched; S, stroma-enriched; B, expressed in both compartments.

Cluster	No. of probe sets	Example genes	Selected GO categories	E	S	B
				%	%	%
1	42	*Aldh3a1, Krt12, Krt13, Scel, Upk1b*	Epithelium development, epithelial cell differentiation	97	0	3
2	15		Sensory organ development, oxygen transport	0	79	21
3	91	*Col14a1, Col3a1, P4ha3*		0	79	21
4	57	**Bnc1**	Positive regulation of transferase activity	74	6	21
5	29	*Adh1, Apod, Aqp1, Cldn10, Dpt, Kera, Krt15*		22	30	48
6	9			0	0	100
7	79	*Bgn, Col1a1, Col1a2, Col5a2, Col6a1, Col6a2, Col6a3, Col8a1, Col11a1, Col12a1, Fmod, Krt19, Krt7, Lama2, Lox, Lum, Plod1*	Regulation of cell adhesion, collagen fibril organization	1	68	30
8	55	*Crabp2, Igf2, Vcan*	Generation of neurons	0	63	37
9	145	*Fbln2, P4ha2, Pitx2, Tcf4, Twist2*	Positive regulation of cell-substrate adhesion and cell differentiation	0	41	59
10	128	*Crabp1, Vim*	Cell-cell adhesion, cell motion, neurogenesis	0	65	35
11	181	*Cldn1, Col5a1, Fn1, Lamc1, Matn2, Nid1, Ogn, P4ha, Sparc*	Positive regulation of cell-substrate adhesion, enzyme linked receptor protein signaling pathway	0	40	60
12	135	*Adh6a, Aqp5, Elf3, Irf1, Itga6, Itgam, Lgals3*	Immune response, tissue remodeling	69	3	27
13	148	*Adh6b, Aqp3, Cldn7, Col17a1, Dsc2, Dsc3, Dsg3, Dsp, Gjb3, Jup,* **Klf4, Klf5**, *Lama3, Lypd3, Ocln, Perp, Ppl, Sfn(14-3-3a), Tkt*	Cell adhesion regulation of cell proliferation	71	1	28
14	72		Extracellular matrix organization, cell-cell signaling	1	26	72
15	65		Muscle tissue development, myofibril assembly	0	46	54
16	40		Neurogenesis	0	59	41
17	303	*Aldh3b2, Cdh1, Elf1, Itgb6, Jdp2, Sdc1, Tjp2, Trp63*	Lipid biosynthetic process	55	3	43
18	62	*Egr1, Krt14*	Sensory perception of light stimulus, epithelium development	3	28	69
19	61			63	0	38
20	174	*Cdo1, Cebpa, Cldn4, Clu, Dcn, Dsg2, Egfr, Fosl2,* **FoxC1**, *Itgb4, Junb, Lamc2, Plec1*	Transmembrane RTK signaling pathway, regulation of cell proliferation, regulation of apoptosis	19	10	71
21	541	*Apoe, Cldn3, Col4a3, Itgb7, Lamb3,* **Pax6**	Small GTPase mediated signal transduction, protein localization	8	3	89
22	697	*Atf6, Itga2, Klf6, Pkp4, Tjp1*	Protein localization, proteolysis in protein catabolic process, vesicle-mediated transport, actin cytoskeleton organization	26	1	74
23	483	*Ctnna1, Ctnnd1,* **Elk4, Hes1**, *Itga3, Itgav, Pkp1, Pkp3, Tcfap2a, Vcl*	Protein transport, vesicle-mediated transport, protein localization, intracellular signaling cascade	30	1	69
24	432	*Aldh1a3, Cgn, Dstn, Tjp3*	Steroid biosynthetic process, oxidation reduction	41	2	58
25	804	*Aldh2, Cebp, Gja1,* **Nfat5, Sp1**	Modification-dependent macromolecule catabolic process, small GTPase signal transduction, intracellular signaling, proteolysis	6	3	91
26	510	**Atf4, Atf5, Atf7**, *Col7a1, Dst,* **Elk3**, *Itgb1, Itgb5, Lama5, P4hb,* **Snai2**	Protein modification process, intracellular signaling cascade, determination of left/right symmetry, phosphorylation	1	11	89
27	165	*Aldh1a1*	Cell cycle, M phase, nuclear division	17	4	79
28	93	**Prox1, Sox2**	Eye development, neuron differentiation, axon guidance, cell morphogenesis involved in differentiation	1	30	69
29	281		Cell cycle, M phase, chromosome organization	4	9	87
30	274		Macromolecular complex subunit organization, chromatin assembly, transmission of nerve impulse	0	22	78
31	333	*Bmp1, Col4a1, Col4a2,* **Gli3**, *Hspg2, Lama1, Lamb2, Plod3*	Small GTPase mediated signal transduction, heart development, regulation of cellular localization, cell adhesion	0	28	72
32	200	*Ctnnd2, Nid2, Tnc,* **Zeb1**	Cell adhesion, actin cytoskeleton organization, axon guidance, negative regulation of transcription from RNA pol II promoter	1	41	58
33	467		RNA processing, chromosome organization, regulation of transcription, mRNA transport	6	3	91
34	404	*Agrn,* **Ldb1**	Cell-cell adhesion, regulation of transcription, chromatin modification	1	14	84
35	427		Sensory perception of chemical stimulus, cell surface receptor linked signal transduction	12	4	83
36	1163	**Cebpe**, *Cldn9, Col19a1, Col4a6,* **Fosb**, *Pkp2*	Sensory perception of chemical stimulus, cell surface receptor linked signal transduction, neg. regulation of molecular function	1	4	95
37	763	*Col4a4,* **Trp73**	Cell surface receptor linked signal transduction, sensory perception of chemical stimulus, defense and wound response	1	3	96
38	431	*Abcg2, Cisd1*	RNA processing, protein folding, DNA metabolic process, response to DNA damage stimulus	21	1	77
39	818	*Cldn14, Col15a1, Col18a1, Ctnna2, Lamc3,* **Trp53**	tRNA metabolic process, mRNA metabolic process, DNA metabolic process, regulation of transcription	0	5	95
40	672	*Adh5, Cisd2, Pin1*	RNA splicing, DNA metabolic process and repair, translation, methylation	4	4	93

skin and is most distinct from E18.5 lung (Fig. 7*A*). Using data from the most differentiated time points (where multiple time points were available), we compared the expression of genes across these eight epithelial tissues, finding that 124 genes were expressed 2-fold or higher in the cornea compared with all of the other tissues (Fig. 7*B* and supplemental Table S2). Of these cornea-enriched genes, about half are members of epithelium-enriched time course clusters, and two-thirds are cornea epithelium-enriched (data not shown). Among these genes were, as expected, previously described genes, such as *Krt12, Upk1b*

Cluster	A	B	C	D	E
	1691	569	624	289	787
	E14.5 E15.5 E17.5 P3 P7 P14 P28	E14.5 E15.5 E17.5 P3 P7 P14 P28	E14.5 E15.5 E17.5 P3 P7 P14 P28	E14.5 E15.5 E17.5 P3 P7 P14 P28	E14.5 E15.5 E17.5 P3 P7 P14 P28
%Enr.					
Member Clusters	1, 13, 17, 20, 21, 23	3, 9, 31	4, 12, 24	5, 7, 11	8, 10, 32, 34
Example Genes	Aldh3a1, Aqp3, Cdh1, Cldn3;4;7, Clu, Col17a1, Dcn, Dsc2;3, Dsg2;3, Dsp, Hes1, Itga3, Itgb4;6;7, Jdp2, Jup, Krt12, Lama3, Lamb3, Lamc2, Lypd3, Ocln, Pkp1;3, Ppl, Scel, Sfn, Tjp2, Tkt, Upk1b, Vcl	Col14al, Col3a1, Fbln2, P4ha2, P4ha3	Adh6a, Aldh1a3, Aqp5, Cgn, Dstn, Irf1, Itga6, Itgam, Lgals3, Tjp3	Adh1, Apod, Aqp1, Bgn, Cldn1;10, Col1a1;a2, Col11a1, Col12a1, Col5a1;a2, Col6a1;a2;a3, Col8a1, Dpt, Fmod, Fn1, Kera, Krt15;19, Lama2, Lamc1, Lox, Lum, Matn2, Nid1, Ogn, P4ha, Plod1, Sparc	Crabp1, Crabp2, Vcan, Vim
TRs	Ehf, FoxC1, Junb, Klf4;5, Pax6, Tcfap2a, Trp63	Pitx2, Tcf4, Twist1, Twist2	Bnc1, Elf3, Nrg1	Aebp1, Ahr, Bmp3, Erg	Igf1, Ldb2, Mitf, Zeb1, Zeb2
Selected GO Categories	protein localization; small GTPase mediated signal transduction; apoptosis; cell adhesion; epidermal cell differentiation	cell adhesion; vascular endothelial growth factor signaling pathway; extracellular matrix organization	immune response; oxidation reduction; cholesterol biosynthetic process	cell adhesion; extracellular matrix organization; collagen fibril organization	cell-cell adhesion; neuron projection development; regulation of transcription

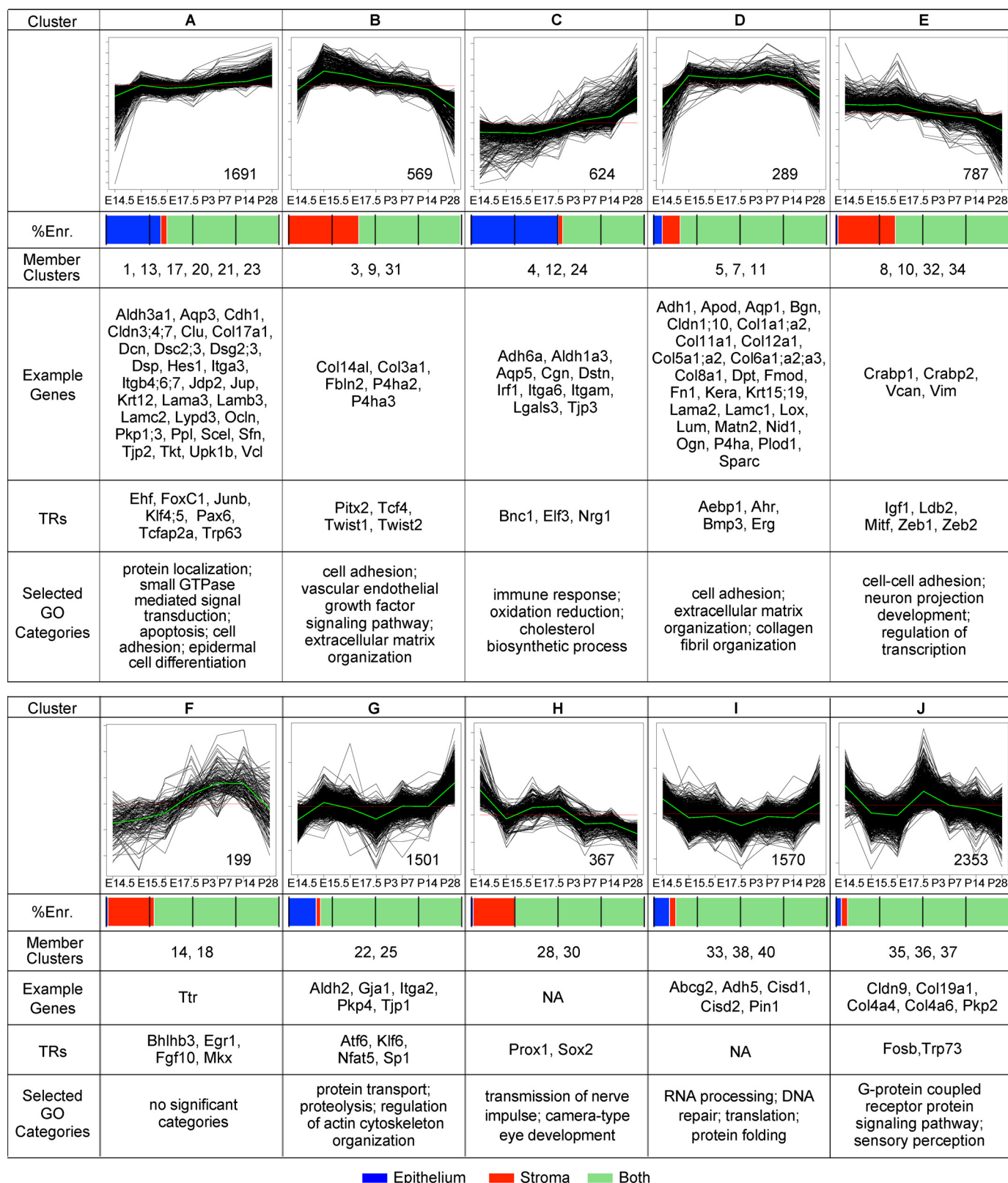| Cluster	F	G	H	I	J
	199	1501	367	1570	2353
	E14.5 E15.5 E17.5 P3 P7 P14 P28	E14.5 E15.5 E17.5 P3 P7 P14 P28	E14.5 E15.5 E17.5 P3 P7 P14 P28	E14.5 E15.5 E17.5 P3 P7 P14 P28	E14.5 E15.5 E17.5 P3 P7 P14 P28
%Enr.					
Member Clusters	14, 18	22, 25	28, 30	33, 38, 40	35, 36, 37
Example Genes	Ttr	Aldh2, Gja1, Itga2, Pkp4, Tjp1	NA	Abcg2, Adh5, Cisd1, Cisd2, Pin1	Cldn9, Col19a1, Col4a4, Col4a6, Pkp2
TRs	Bhlhb3, Egr1, Fgf10, Mkx	Atf6, Klf6, Nfat5, Sp1	Prox1, Sox2	NA	Fosb,Trp73
Selected GO Categories	no significant categories	protein transport; proteolysis; regulation of actin cytoskeleton organization	transmission of nerve impulse; camera-type eye development	RNA processing; DNA repair; translation; protein folding	G-protein coupled receptor protein signaling pathway; sensory perception

■ Epithelium ■ Stroma ■ Both

FIGURE 5. **Time course clustering of cornea developmental genes reveals distinct gene expression patterns associated with epithelium and stroma.** Shown are the expression profiles of superclusters (*A–J*) that were formed by combining similar *k*-means clusters (see Fig. 3); the membership of individual clusters is indicated *below* each supercluster. The number of probe sets; the relative proportion (%*Enr.*) of epithelium-enriched genes (*blue*), stroma-enriched genes (*red*), and genes expressed in both compartments (*green*); example genes; transcriptional regulators (*TRs*); and top GO categories are indicated. For temporal expression graphs, the *x axis* shows the developmental time point, and the *y axis* shows $\log_2$ expression; each *tick mark* represents 1-fold. *Red line*, 0. *Green line*, average expression value at each time point for all genes in the cluster.
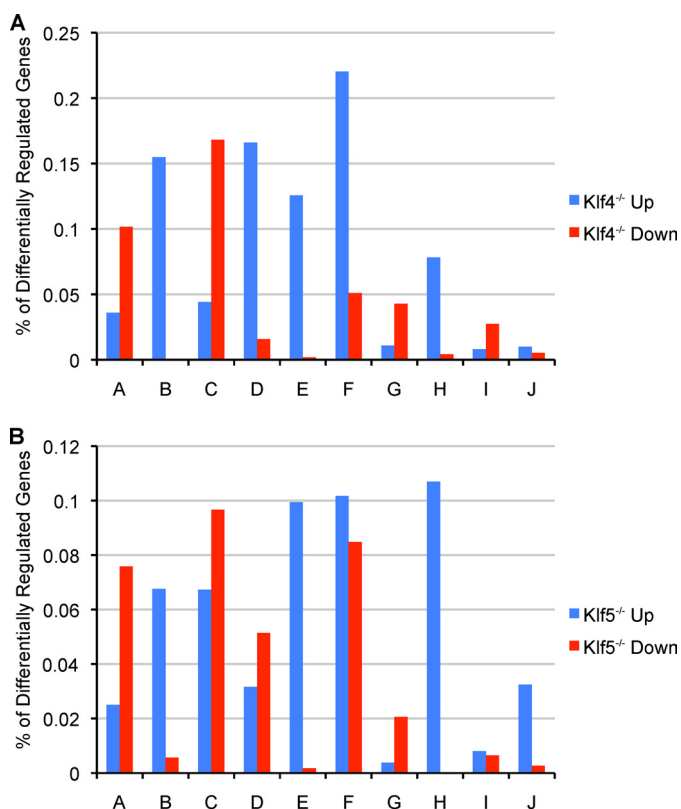
FIGURE 6. **Differentially regulated genes in *Klf4*$^{-/-}$ and *Klf5*$^{-/-}$ corneas overlapped with the developmental superclusters (see Fig. 5).** *A*, percentage of genes in each supercluster affected by the cornea deletion of *Klf4*. *B*, percentage of genes in each supercluster affected by the cornea deletion of *Klf5*. *Up*, up-regulated genes in response to gene deletion. *Down*, down-regulated genes in response to gene deletion.

(57), and *Slurp1* (67), but also the transcription factor *Ehf* with unknown functions in the cornea. We conclude that relatively few genes are highly enriched in cornea compared with other epithelia and that these genes are likely to carry out cornea-specific functions.

Aging-associated Gene Expression Changes in the Cornea; Enrichment of Epithelium- and Stroma-enriched Genes—To identify genes with significant changes in expression during aging, we utilized Cyber-T (16, 17) to compare cornea mRNA expression between young adult (average of P28 and P60) and old (2-year) mice. At $p < 0.01$, 608 genes (664 probe sets, 2.5% of the transcriptome) are differentially expressed (Table 3 and supplemental Table S3). This compares with 10,209 genes (45% of the transcriptome) differentially expressed during cornea development, indicating that a much smaller portion of the genome exhibits dynamic expression changes in aging than in development. Furthermore, as found in other aging studies, most expression changes were less than 2-fold, whereas dramatic expression changes were common in development. Analyzing 43 aging gene expression data sets from 32 mouse tissues available in GEO2R (20, 21), we found that the portion of the transcriptome changing in aging varies from less than 1% up to 24% of transcripts, with the majority of tissues showing changes in less than 10% of the transcriptome (Table 4). With 2.8% of probe sets changing in cornea aging, the cornea falls into a group of tissues with a relatively modest change in aging-related gene expression.

In the cornea aging transcriptome, 10 and 17% of transcripts are epithelium- and stroma-enriched, respectively, representing a 1.5- and 3.2-fold enrichment of epithelial and stromal transcripts, respectively, compared with that found in development. These data demonstrate that stroma/epithelium-specific genes are preferentially affected during aging and that aging gene expression changes are greater in the stroma than in the epithelium. However, we did identify three cornea- and epithelium-enriched genes that are significantly differentially regulated, *Slurp1* (-1.59-fold), *1600014C10Rik* (-7.41-fold), and *Ehf* (1.25-fold), suggesting that they may be of importance in cornea epithelial aging.

The 608 aging transcripts were grouped into 16 distinct patterns by hierarchical clustering (Fig. 8*A*; only the nine clusters with significant GO enrichment are shown). We found epithelium-related GO terms, such as epithelial cell differentiation and lipid biosynthetic process, in clusters with increasing expression during aging, whereas stroma-related terms, such as cell adhesion and ECM-receptor interaction, were found in clusters with decreasing expression during aging. We also observed a decreasing expression of translation- and ribosome-related genes and an increasing expression in blood vessel development-related genes. These categories suggest that increased epithelial cell differentiation and decreased matrix expression, perhaps corresponding to the previously described increase in stromal collagen spacing with aging (68), are inherent to cornea aging.

Comparing the differentially expressed genes in aging with those differentially expressed in development, we found 382 genes in common, whereas 226 genes were uniquely changing in aging (Fig. 8*B*). The genes commonly altered in development and aging are associated with cell adhesion and regulation of cell morphogenesis (Fig. 8*C*), processes that are important in both development and aging. The genes changing uniquely in aging are enriched for translation-related genes and were not epithelium- or stroma-enriched; most of these translation-related genes are down-regulated. Interestingly, recent work in mice has demonstrated that down-regulation of translation pathways results in increased longevity (69). This reduced translation in the cornea may contribute to the functional maintenance of the cornea in aged mammals.

Next, we asked whether previously defined aging-regulated genes from other tissues also change in the cornea. We compared differentially regulated genes in the aging cornea with those in 42 other aging data sets from a variety of tissues (Table 4). To a large extent, unique genes were expressed in each one of these tissues. However, the aging transcriptomes of tail skin, cochlea, and lungs were more similar to cornea than predicted by random chance ($p < 0.01$), whereas several aging transcriptomes were less similar to cornea than predicted, including those from myoblasts, heart ventricle, muscle, bone marrow, and brain. We found that 479 genes were differentially expressed in the cornea and in at least one other aging gene expression data set, with relatively few altered across numerous tissues (Fig. 8*D*). The top common genes represent several known age-regulated pathways, such as cell adhesion, ion transport, and cell death, suggesting that these particular genes
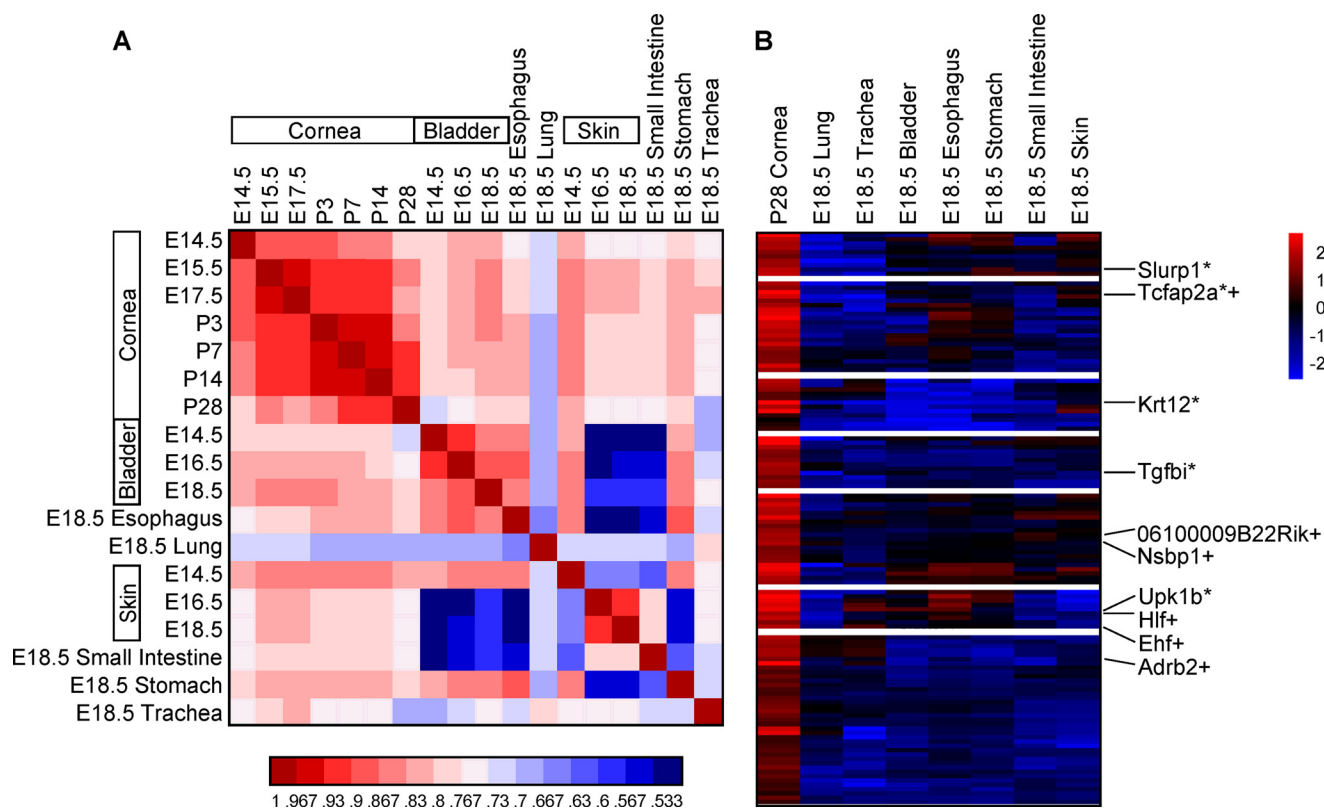
FIGURE 7. **Comparison of the whole genome expression profiles of various mouse epithelial tissues.** *A*, gene distance matrix comparing correlation of global expression profiles of developmental cornea time points with the indicated epithelial tissues. The correlation scale is indicated *below*. *B*, heat map depicting top corneal enriched genes. A comparison of the most differentiated time point or E18.5 in each tissue found 124 genes to be at least 2-fold higher expressed in the cornea than in all other tissues tested in these experiments. *, known cornea markers; +, transcription factors.

may be important aging regulators in their respective pathways, regardless of the tissue in which they are expressed.

ChIP-seq and Functional Studies Identify EHF as a Regulator of Cornea Epithelial Cell Identity—To identify potential new regulators of cornea epithelial differentiation, we decided to focus on the Ets transcription factor EHF. The *Ehf* transcripts are progressively up-regulated during development, remaining highly expressed during adulthood with a limited (~1.3-fold) but significant increase in expression as aging progresses (Fig. 9*A*). The EHF protein is selectively expressed within nuclei of the mouse cornea epithelium (Fig. 9*B*), and in the cornea, *Ehf* transcripts are expressed at a greater than 2-fold higher level than in the other epithelial tissue we profiled (Fig. 9*C*).

The localization of *Ehf* in supercluster A with numerous cornea epithelial differentiation genes (Fig. 5) and its preferential expression in the epithelium (Fig. 9*D*) suggested that it is a potential regulator of cornea epithelial cell differentiation. To identify direct EHF targets, we performed ChIP-seq on cornea epithelium isolated from 3-month-old mouse corneas. At a false discovery rate of 5%, 15,384 EHF ChIP-seq peaks were called against the input control. Of these, 5570 peaks were found in the proximal promoter regions of genes, defined as a 3-kb window from 2 kb upstream to 1 kb downstream of transcription start sites (Fig. 9*E*). GO analysis of genes bound by EHF revealed a highly significant enrichment for transcriptional regulation (Fig. 9*F*); in particular, EHF bound the promoters of other Ets genes like *Ets1*, *Ets2*, and Ets2 repressor factor *Erf* (data not shown). Additional significantly enriched

gene ontology categories included signaling, cell migration, and epithelium morphogenesis (Fig. 9*F*). The top enriched peaks include genes such as wound healing-related *Plaur* (70) and *Tcf4*, recently implicated in limbal stem cell maintenance (71) (Fig. 9*G*).

De novo motif searches on the 1000 most highly enriched EHF peaks identified, as expected, an enrichment of a motif similar to the core Ets motif (Fig. 9*H*). Intriguingly, a motif matching the binding site for KLF4, a transcription factor involved in cornea epithelial differentiation, was also highly enriched in these EHF ChIP-seq peaks (Fig. 9*I*), suggesting that there may be co-regulation of target genes and overlap in biological functions between these two transcription factors. This finding is further supported by the observation that ~30% of genes affected by knock-out of *Klf4* in the cornea (72) have an EHF peak within 20 kb of their transcription start site (data not shown).

To determine what additional cofactor motifs might be present within the full data set of EHF ChIP-seq peaks, we performed directed motif searches using the Cistrome motif-based interval screener with position-specific scoring matrix. This search revealed significant enrichment of the EHF, ETS2, PAX6, KLF4, and KLF5 motifs within the EHF peaks when compared with negative control regions of identical size (Fig. 9*J*). The KLF5 motif was most highly enriched and was found in ~30% of EHF peaks. Interestingly, the Ets motif associated with ETS2 was more highly enriched within the EHF peaks than the published EHF motif. These two motifs are similar, sharing the

TABLE 3

List of the genes most up-regulated in cornea during aging

Gene symbol, name, *p* value, and -fold change compared with young adulthood (P28) is indicated.

Gene symbol	Gene description	*p* value	Change
			-fold
Sytl2	Synaptotagmin-like 2	0.000	13.22
Cyp1b1	Cytochrome P450, family 1, subfamily b, polypeptide 1	0.001	9.15
Defb14	Defensin β14	0.007	7.10
Serpina3n	Serine (or cysteine) peptidase inhibitor, clade A, member 3N	0.001	5.54
Spink5	Serine peptidase inhibitor, Kazal type 5	0.000	4.97
Napepld	*N*-Acyl phosphatidylethanolamine phospholipase D	0.000	4.12
Casp1	Caspase 1	0.009	3.94
Ly6e	Lymphocyte antigen 6 complex, locus E	0.001	3.60
Cmah	Cytidine monophospho-N-acetylneuraminic acid hydroxylase	0.006	3.35
Fetub	Fetuin β	0.005	3.33
EG665378	Predicted gene, EG665378	0.006	3.29
EG665378	Predicted gene, EG665378	0.003	3.28
Ptpn22	Protein-tyrosine phosphatase, non-receptor type 22 (lymphoid)	0.000	3.27
Csprs	Component of Sp100-rs	0.005	2.99
Csprs	Component of Sp100-rs	0.005	2.87
Klk10	Kallikrein-related peptidase 10	0.001	2.84
Csprs	Component of Sp100-rs	0.007	2.78
Prss22	Protease, serine, 22	0.006	2.70
Olfr742	Olfactory receptor 742	0.001	2.68
S100a7a	S100 calcium-binding protein A7A	0.005	2.60
C3	Complement component 3	0.001	2.59
Ceacam19	Carcinoembryonic antigen-related cell adhesion molecule 19	0.005	2.53
Car5b	Carbonic anhydrase 5b, mitochondrial	0.002	2.50
Tfrc	Transferrin receptor	0.008	2.44
Snhg1	Small nucleolar RNA host gene (non-protein coding) 1	0.001	2.43
Ecm1	Extracellular matrix protein 1	0.000	2.37
Tas2r117	Taste receptor, type 2, member 117	0.001	2.43
Vgll3	Vestigial like 3 (Drosophila)	0.002	2.31
Srd5a1	Steroid 5 α-reductase 1	0.000	2.28
Elf3	E74-like factor 3	0.005	2.19
Aldoc	Aldolase C, fructose-bisphosphate	0.000	2.19
Chi3l3	Chitinase 3-like 3	0.004	2.19
Pdxk	Pyridoxal (pyridoxine, vitamin B6) kinase	0.000	2.19
Errfi1	ERBB receptor feedback inhibitor 1	0.008	2.14
Blnk	B-cell linker	0.007	2.11
Ptgs1	Prostaglandin-endoperoxide synthase 1	0.001	2.09
Stambp	Stam-binding protein	0.002	2.07
Hsd17b7	Hydroxysteroid (17-β) dehydrogenase 7	0.002	2.04
ENSMUSG00000053531	Predicted gene, ENSMUSG00000053531	0.001	2.00

core Ets sequence within their respective motifs, and both EHF and ETS2 fall into the same class in an analysis where Ets factors were grouped by the sequence similarity of their motifs (73). It is possible that EHF binding specificity may vary depending on the context of the binding and the cofactors with which it interacts. PAX6 was also enriched in a small but significant fraction of EHF peaks, suggesting that PAX6 and EHF may co-regulate a subset of their target genes. Furthermore, we found that the PAX6 and Ets motifs co-occurred within peaks, as did the KLF and Ets motifs. In contrast, there was no overlap between PAX6 and KLF motifs, supporting the idea that EHF interacts separately with PAX6 and KLF factors to regulate different subsets of gene targets. Similar to recent studies on other transcription factors (74, 75), we found a significant fraction of EHF peaks without the canonical EHF or Ets motifs. In these instances, EHF may be recruited through protein-protein interactions rather than binding the DNA directly, or under *in vivo* conditions, like in our experiment, EHF may bind to several different motifs in a context-dependent manner.

To assess the relationship between gene expression and EHF binding, we ranked the gene expression data from the isolated mouse cornea epithelium at P28 and divided it into quintiles based on expression levels. EHF peaks were most enriched in the most highly expressed quintile and least enriched in the quintile with the lowest expressed genes, consistent with a role for EHF in regulating cornea epithelial identity by increasing the expression of differentiation genes (Fig. 9*K*).

To identify genes regulated by EHF, we knocked down *EHF* (Fig. 10*A*) in primary human cornea epithelial cells and assessed global gene expression with microarrays. We found nearly 500 differentially regulated genes, 365 down-regulated and 132 up-regulated, suggesting that in the cornea epithelium, EHF acts predominantly as a transcriptional activator. Overlapping the EHF-regulated genes with the mouse superclusters (Fig. 10*B*), we observed that the genes belonging to the epithelial superclusters (A, C, and G) were predominantly down-regulated upon *EHF* knockdown, providing further evidence that EHF is primarily a transcriptional activator of cornea epithelium differentiation genes. Interestingly, genes up-regulated after *EHF* knockdown were overrepresented in certain stromal superclusters (B, E, and H), suggesting that EHF also suppresses expression of stromal genes in cornea epithelial cells. Consistent with these findings, GO analysis of down-regulated genes in response to *EHF* knockdown revealed an enrichment of ectoderm development/epithelial differentiation and response to wounding, including genes in the epidermal differentiation complex (cytoband 1q21–1q22) (76) (Fig. 10*C*). In contrast, GO analysis of up-regulated genes in response to *EHF* knockdown, identified angiogenesis and blood vessel morphogenesis, fur-

The Ets Factor EHF as a Regulator of Epithelial Cell Fate

TABLE 4

Aging data sets used in aging tissue comparison

Tissue analyzed, age of mice, number of genes in the data set (or on the chip used), overlap with cornea, and representation factor compared with the cornea are listed. NA, not available.

Tissue	Age(s)	Age(s)	GSE[a]	No. of data rows	Rows $p < 0.01$	Probe sets changing	No. of rows with annotation	Overlap with cornea	Representation factor	p value
						%				
Striatum	1 month[b]	24 month[b]	GSE9909	8932	11	0.1	10	0	0.0	0.476
Hippocampus	1 month[b]	24 months[b]	GSE9909	8932	24	0.3	24	0	0.0	0.168
Bone marrow	1 month[b]	24 months[b]	GSE9909	8932	31	0.3	31	0	0.0	0.100
Muscle	1month[b]	2 months[b]	GSE9909	8932	38	0.4	37	2	0.8	0.500
Cerebrum	1month[b]	24 months[b]	GSE9909	8932	53	0.6	53	1	0.3	0.099
Kidney	1month[b]	24 months[b]	GSE9909	8932	53	0.6	53	1	0.3	0.099
Liver	1month[b]	24 months[b]	GSE9909	8932	94	1.1	94	2	0.3	0.031
Prostate-dorsal lobe stroma	4 months	20–24 months[b]	GSE21542	45,186	498	1.1	247	5	0.8	0.374
Spleen	1 month[b]	24 months[b]	GSE9909	8932	112	1.3	112	6	0.7	0.301
RPE	2 months	24 months	GSE565	1185	14	1.3	15	1	0.1	5.28E-04
Heart	1 month[b]	24 months[b]	GSE9909	8932	143	1.6	143	6	0.6	0.106
Lungs	2 months	18 months	GSE6591	45,101	806	1.8	679	30	1.7	0.004
Spinal Cord	1 month[b]	24 months[b]	GSE9909	8932	179	2.0	179	4	0.3	0.003
Hippocampus	3.5 months	18 months	GSE29075	45,281	936	2.1	785	30	1.5	0.024
Hematopoietic stem cells	2–3 months	22–24 months	GSE4332	45,101	944	2.1	829	23	1.1	0.410
Cerebellum	1 month[b]	24 months[b]	GSE9909	8932	222	2.5	222	5	0.3	0.001
Heart ventricle	4 weeks	12 months	GSE75	12,654	331	2.6	312	12	0.8	0.308
Hippocampus	2 months	15 months	GSE5078	11,488	303	2.6	290	12	0.8	0.276
Cornea	1–2 months	24 months	GSE43155	23,887	639	2.7	639 or 586[c]	639	35.2	0.000
Adrenals	1 month[b]	24 months[b]	GSE9909	8932	252	2.8	252	9	0.5	0.012
RPE	2 months	24 months	GSE565	1185	34	2.9	34	2	0.1	3.33E-08
Prostate-anterior lobe stroma	4 months	20–24 months	GSE21542	45,176	1457	3.2	697	18	1.0	0.454
Bone marrow adipocyte	6 months	18 months	GSE25905	35,556	1239	3.5	1239	42	1.2	0.136
Oocytes-GV	6 weeks	66 weeks	GSE11667	45,101	1597	3.5	1405	27	0.7	0.053
Gonads	1 month[b]	24 months[b]	GSE9909	8932	355	4.0	355	9	0.4	8.88E-05
Lungs	2 months[b]	18 months	GSE6591	45,101	1793	4.0	1455	52	1.4	0.013
Primary myoblasts	8 months	23 months	GSE273	11,488	506	4.4	476	16	0.7	0.043
Oocytes-MII	5–6 weeks	42–45 weeks	GSE1646	21,939	1029	4.7	890	15	0.6	0.033
Eye	1 month[b]	24 months[b]	GSE9909	8932	429	4.8	429	10	0.3	5.55E-06
Muscle, skeletal	5 months	25 months	GSE6323	22,690	1126	5.0	1046	36	1.3	0.055
Rod photoreceptor	1.5 months	12 months	GSE22317	45,101	2683	5.9	2019	53	1.0	0.500
Lung	1 month[b]	24 months[b]	GSE9909	8932	557	6.2	557	21	0.5	3.99E-04
Oocytes-MII	6 weeks	66 weeks	GSE11667	45,101	2964	6.6	2530	74	1.1	0.159
Cochlea	4 weeks	45 weeks	GSE35234	45,291	3812	8.4	3282	88	1.0	0.404
Thymus	1 month[b]	24 months[b]	GSE9909	8932	936	10.5	936	30	0.4	4.17E-08
Cochlea	7 weeks	36 weeks	GSE6045	22,626	3251	14.4	2733	101	1.4	1.73E-04
Tail Skin	5 months	30 months	GSE35322	45,101	6923	15.3	403	154	1.2	0.002
Peripheral adipocyte	6 months	18 months	GSE25905	35,556	6418	18.1	6418	171	0.9	0.165
Neocortex	5 months	30 months	GSE13120	45,037	8769	19.5	6822	192	1.1	0.107
Kidney	10–12 weeks	14 months	NA (Ref. 23)	230	45	19.6	45	0	0.0	NA
Thymocytes	1 month	24 months	GSE15945	41,534	8158	19.6	6001	174	1.1	0.054
Heart	10–12 weeks	14 months	NA (Ref. 23)	276	58	21.0	58	3	NA	NA
Brain	10–12 weeks	14 months	NA (Ref. 23)	171	41	24.0	40	0	0.0	NA

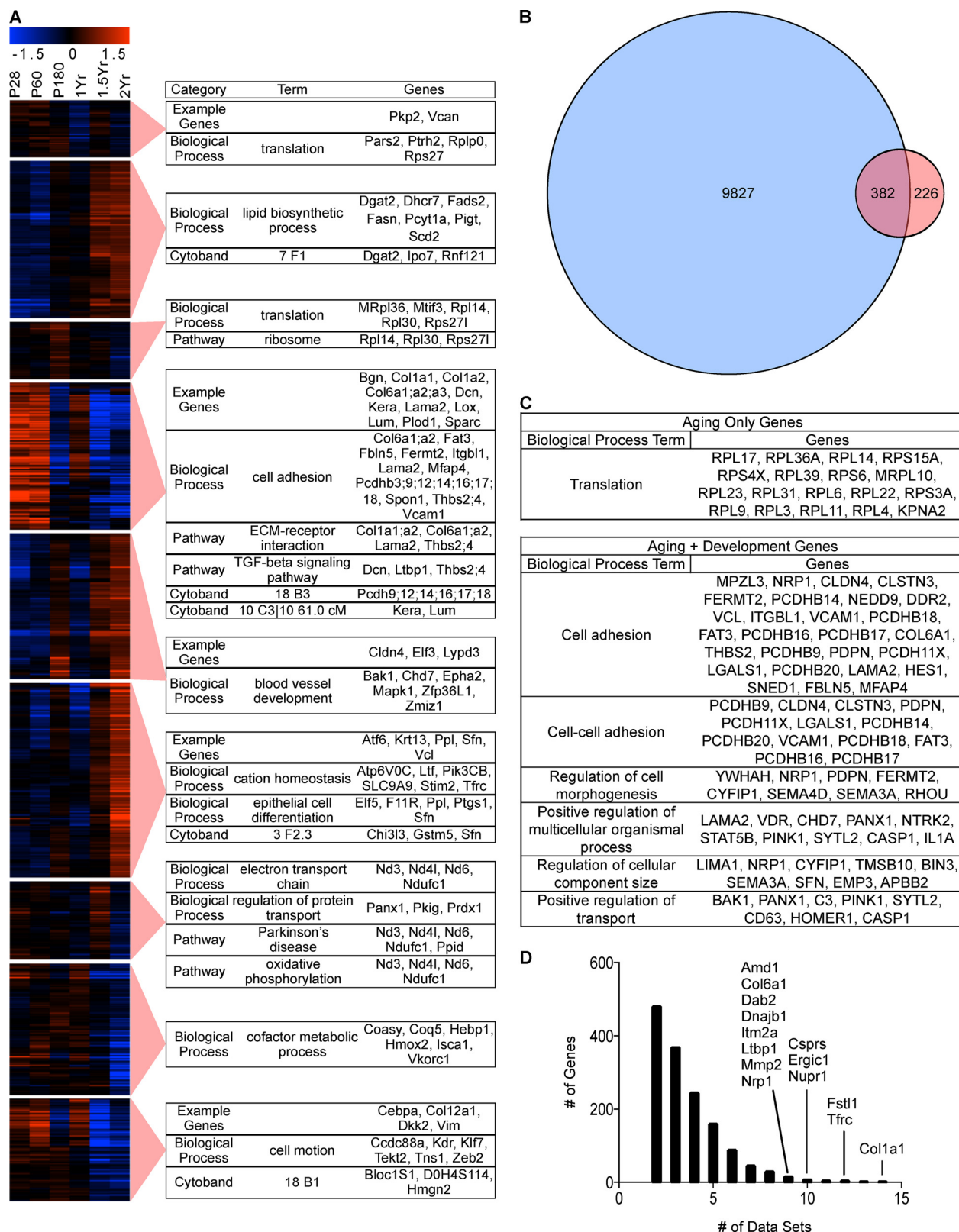[a] Only control samples at the indicated time points from the these studies were utilized.

[b] AGEMAP analysis; four time points were utilized: 1, 6, 16, and 24 months.

[c] For the cornea data set, 586 gene symbols/Unigene IDs were used for all data sets except for the experiments on the Mouse Gene 1.0ST and NIA Mouse 17K platforms, where 639 genes were used.

ther supporting the notion that EHF represses genes that could compromise corneal clarity.

To study the functional effects of EHF binding, we overlapped the genes affected by *EHF* knockdown with genes that have a linked EHF peak, defined as 20 kb upstream and throughout the gene's body. About 50% of genes affected by *EHF* knockdown have a linked EHF peak (Fig. 10*D*). These genes are enriched for epithelial differentiation-associated GO categories, including tissue morphogenesis, epithelial development, regulation of phosphorylation, and negative regulation of proliferation (Fig. 10*E*). With respect to the quintiles of ranked epithelial gene expression, genes with an EHF peak that were down-regulated by the knockdown tended to fall into the highly expressed epithelial quintiles, whereas genes with an EHF peak up-regulated by the knockdown tended to fall into the lower expressed quintiles (Fig. 10*F*). This suggests a role for EHF in promoting epithelial identity, primarily through the activation of genes in cornea epithelium but also through the repression of non-epithelial genes.
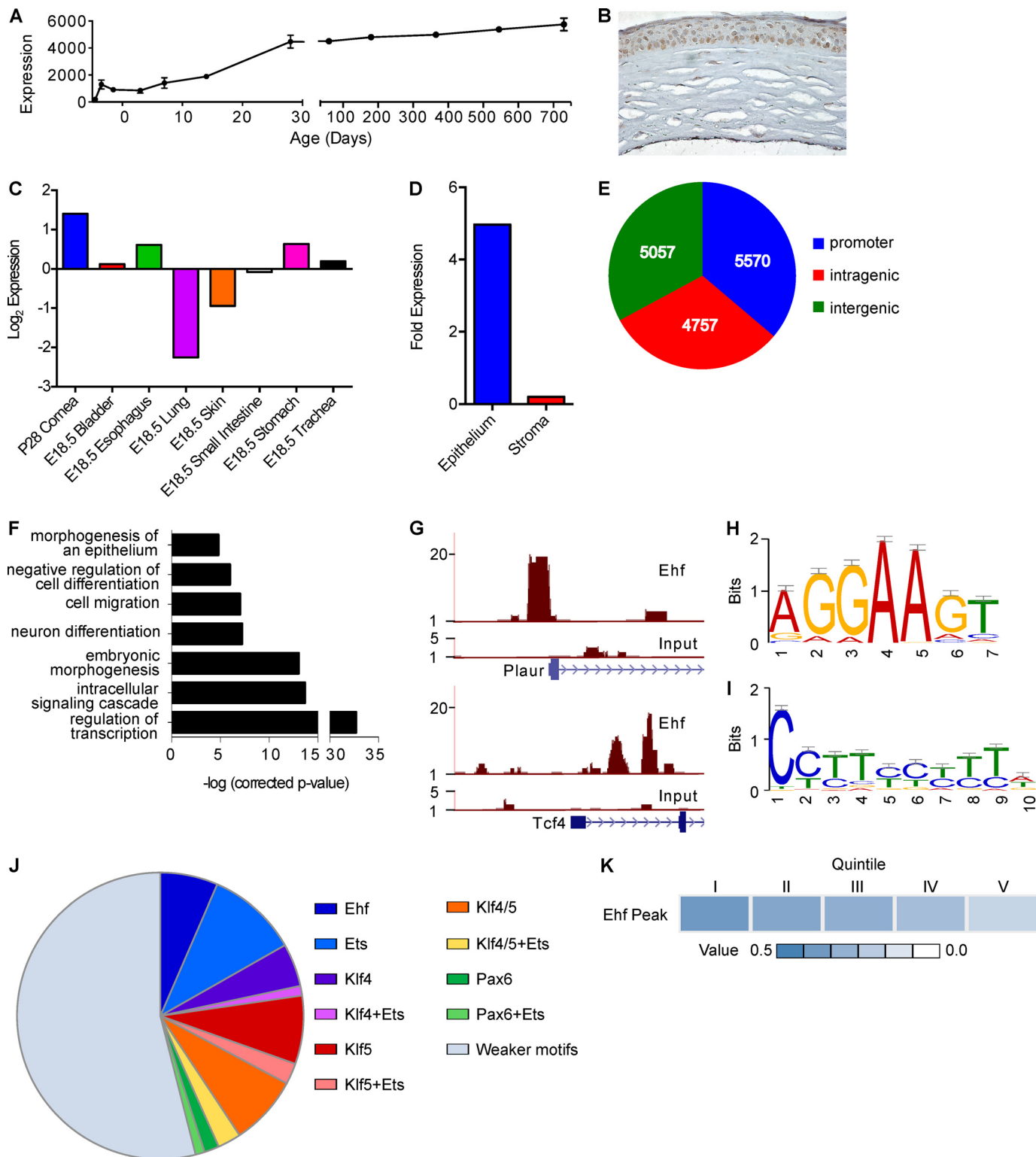
To identify potential regulatory patterns, we determined where the ChIP-seq and siRNA data fell across the temporal expression clusters (Fig. 10*G*). Whereas the genes with ChIP-seq peaks in their proximity distributed fairly evenly across the clusters, when overlapped with the siRNA data, there was a significant difference in the number of peaks overlapping up-regulated *versus* down-regulated genes within the individual clusters. All of the strong epithelial superclusters (A, C, and F), have EHF peaks near genes down-regulated by *EHF* knockdown, suggesting that at these loci, EHF binding is strongly associated with gene activation. Stromal superclusters E and H and weak stromal supercluster D had EHF peaks near genes that are up-regulated by knockdown of *EHF*, suggesting repression of stromal or non-epithelial genes. The equally enriched superclusters I and J were mostly composed of genes not bound by EHF. These data further support the idea that EHF acts in the cornea epithelium to activate epithelial genes and repress non-epithelial genes, like those found in stroma-enriched clusters.

FIGURE 8. **Analysis of aging gene expression points to alterations in unique and common aging functions in cornea.** *A*, heat maps showing the expression of genes exhibiting change in expression during cornea aging; these genes fall into nine distinct clusters based on temporal expression patterns. For each cluster, example genes, top significant biological processes, cytobands, and pathways are shown. *B*, overlap of developmentally regulated (*blue*) and aging-regulated (*red*) genes. *C*, GO analysis of genes differentially regulated in aging only and genes differentially regulated in both development and aging. *D*, comparison of cornea aging genes to aging genes in other mouse tissues identified in 42 publicly available mRNA expression data sets. The *y* axis shows the number of aging genes in common between cornea and other tissues; the *x* axis shows the number of data sets that have common genes. We found that 479 cornea aging genes are present in at least one other aging data set. The graph shows the gene symbols for cornea aging genes changing in nine or more data sets; such genes probably reflect aging processes common to many tissues.

The Ets Factor EHF as a Regulator of Epithelial Cell Fate

The specific genes that are down-regulated after *EHF* knockdown point to multiple possible roles of EHF in the epithelium. Several genes encoding keratin-cross-linking SPRR proteins are down-regulated, suggesting a role in barrier function (77). Alternatively, the down-regulation of anti-angiogenic SERPIN genes (78, 79) and the up-regulation of angiogenic genes in the epithelium points to a role for EHF in maintenance of corneal transparency through suppression of angiogenic factors. Another possible role of EHF is in immune response of the cornea. Genes in the TNF superfamily and the SAA family and *IL19* are all down-regulated. TNF genes are regulators of inflammation and apoptosis (79), whereas SAA proteins and IL19 are both responsive to bacterial lipopolysaccharides (80, 81). In sum, our data suggest that EHF regulates cornea epithe-

lial cell identity by activating differentiation genes and repressing non-epithelial genes.

DISCUSSION

Our genome-wide cornea mRNA expression study is the first performed over the lifetime of the mouse, providing a detailed, continuous profile of whole mouse cornea transcript expression through embryonic and early postnatal development into aging. Previous work compared whole cornea mRNA expression in P9 and 6-week-old mice, identifying the most abundantly expressed transcripts, transcriptional regulators, and enriched gene groups in the developing and adult mouse cornea (11). Another study compared cornea stroma mRNA expression from P10 and adult mice with that of cultured keratocytes, fibroblasts, and myofibroblasts, revealing a role for the stroma in maintenance of transparency as well as in barrier protection during times of infection or injury (10). A third study compared whole cornea mRNA expression in P10 and 7-week-old mice with that of lens and tendon, defining cornea-enriched genes compared with the lens and tendon (9). The comprehensive picture of cornea gene expression in our study provides new insights into both cornea development and aging, helps define the transition point between development and adulthood, and identifies new pathways and genes involved in development and aging. In particular, we have identified the Ets factor EHF as a promoter of cornea epithelial cell identity.

A Cornea Gene Expression Switch at the Juncture of Development and Adulthood—The timing for the completion of cornea development remains controversial. Based on morphology, early electron microscopic studies argued that development is completed at eye opening (P14) (8, 82). In contrast, an *in vivo* confocal microscopy study reported that epithelial and stromal development is concluded by P30 (83), whereas another study reported that the cornea did not fully mature until 2 months of age (84). A global comparison of the gene expression profiles in our study through PCA argues that cornea development ends between P14 and P28 (Fig. 1*D*). This conclusion is also supported by the underlying structure in our data set, where over 1000 genes show a prominent switch in expression between P14 and P28 (Fig. 2*B*). Among these genes, we identified a group of myofibril assembly transcripts that are expressed in development and not aging. Although actins and myosins have been studied in the cornea, where they were found to play roles in cell migration, regulation of cell shape, and wound healing (85–87), we have identified several transcripts in this group with unknown roles in the cornea, including actins α1 (*Acta1*) and γ1 (*Actg1*) and myosins heavy chain 10 (*Myh10*) and light chain

2 (*Myl2*) (Fig. 2*C*), which were previously linked to cardiac and/or skeletal muscle; MYH10 was recently shown to coordinate collagen translation in mouse embryonic fibroblasts (88). These findings suggest that these genes associated with striated muscle may play additional roles in the developing cornea, potentially in collagen fibril organization and/or epithelial cell migration.
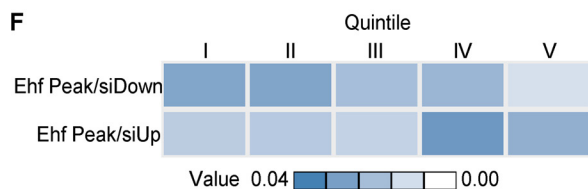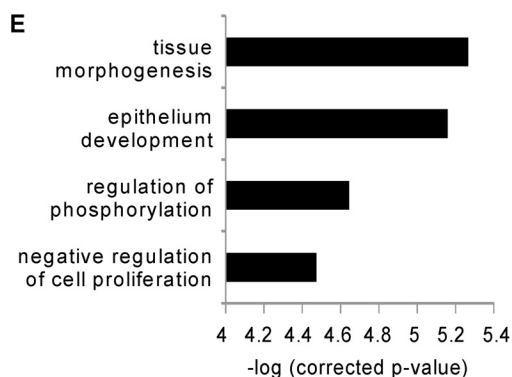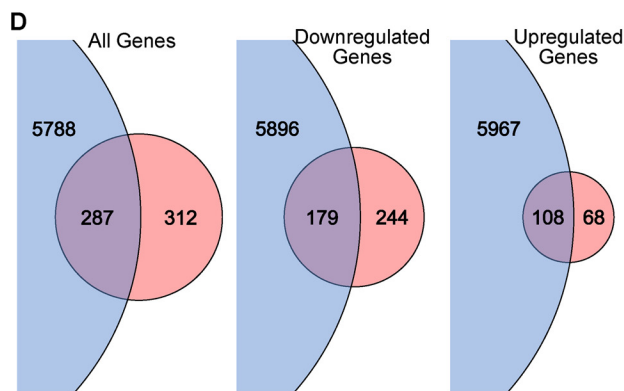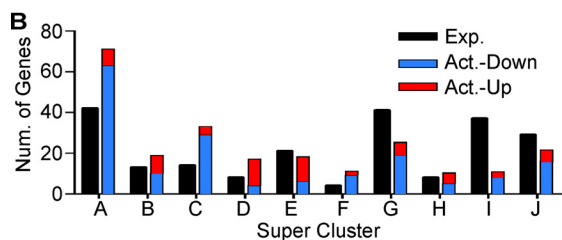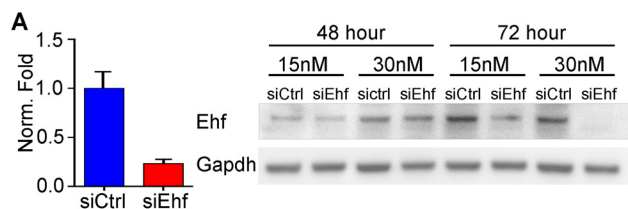
Gene Expression in Corneal Development—Previous studies have demonstrated that co-expression of genes is often a characteristic of co-regulated genes (89, 90), particularly among genes that are highly expressed and/or co-regulated by multiple transcription factors. Thus, the identification of a set of temporal gene expression clusters in development (Fig. 3) allows us to make inferences about potential transcriptional relationships in the cornea that could not have been discovered with previous cornea microarray studies. The inclusion of expression data from separated epithelium, separated stroma, and other epithelial tissues further refined the data. Validating this approach, we observed that known target genes of the transcription factors KLF4 and KLF5 (58, 59, 72) were located within the same supercluster as *Klf4* and *Klf5*. Our clustering approach allowed us to gain insights into the previously published gene expression data for mice deleted for *Klf4* and *Klf5* in the cornea. Incorporating information about cluster membership into the list of genes affected by the *Klf4* and *Klf5* deletions demonstrates that these factors primarily activate genes in epithelial enriched clusters, whereas many of the genes up-regulated in response to gene deletion reflect the previously described secondary changes in the stroma.

The data are also useful for gaining insights into cornea stroma development. Thus, we found that *Twist2*, which has a known role in stroma development (64), belongs to stroma-enriched supercluster B. Interestingly, the family member *Twist1*, which has an unknown function in cornea, also falls into supercluster B, raising the possibility that it also is involved in stroma development, perhaps jointly with *Twist2* (91).

Aging in the Cornea—Our analysis of aging in the cornea identified 608 differentially regulated transcripts representing 2.8% of the transcriptome. The gene expression changes during cornea aging are modest compared with development, consistent with reports on other aging tissues (22). Aging genes grouped into broad clusters by overall trends of down-regulation or up-regulation (Fig. 4*A*). The enrichment of genes within each cluster captured several different pathways commonly regulated in aging, such as lipid biosynthetic process, cell adhesion and TGFβ signaling, blood vessel development, electron

FIGURE 9. **ChIP-seq on mouse cornea epithelium identifies the Ets factor EHF as a potential regulator of cornea epithelial gene expression.** *A*, expression of *Ehf* in mouse cornea over the lifetime of the mouse. *Ehf* belongs to supercluster A, which contains known cornea epithelial markers and regulators, including *Klf4* and *Klf5*. *B*, expression of the EHF protein by immunohistochemistry in adult mouse cornea epithelium; expression is limited to epithelial cells. *C*, *Ehf* transcript expression across mouse epithelial tissues; expression is highest in cornea, but also relatively high in esophagus and stomach. *D*, *Ehf* transcript expression in cornea epithelium and stroma. Consistent with the immunohistochemistry data in *B*, transcript expression is essentially limited to the epithelium. *E*, the number of EHF ChIP-seq peaks that are bound at the promoter of genes, within genes (intragenic), or between genes (intergenic). *F*, GO analysis of EHF promoter-bound genes. *G*, two example genes bound by EHF. *H*, *de novo* motif analysis of EHF-bound peaks identified a motif similar to the common Ets motif. *I*, *de novo* motif analysis of EHF-bound peaks also identified a motif similar to the KLF4 motif. *J*, motif analysis of all EHF ChIP-seq peaks showing the proportion of peaks containing the EHF, KLF4, KLF5, and/or PAX6 binding motifs within the promoter. KLF4 and KLF5 motifs are commonly identified in EHF-bound regions, sometimes in addition to an Ets motif. *K*, the frequency of EHF peaks (scale indicated *below*) in relation to cornea epithelial expression levels of the bound gene, arranged in quintiles with *I* being highest expression and *V* being lowest expression. The frequency of EHF peaks correlates positively with the cornea epithelial expression level of genes.

A

B

C

	siRNA - Ehf	
	All genes - p < 0.01 - 497	
Category	**Term**	**Genes**
Cytoband	1q21-q22	SPRR2D, SPRR1B, SPRR2A, SPRR2B, SPRR3, SPRR2G, SPRR2E
Cytoband	1q21	MUC1, S100A8, PGLYRP4, S100A7, PGLYRP3, S100A9, ARNT, S100A12, HIST1H4H
Biological Process	ectoderm development	KLK7, PPARD, PTGS2, FOXA2, S100A7, CRABP2, KLK5, FOXN1, SPRR2G, GRHL3, SPRR2E, JAG1, KRT34, SCEL, EREG, SPRR2D, SPRR1B, SPRR2A, OVOL1, SPRR2B, CNFN, FOXE1, SPRR3, WNT7A
Biological Process	epithelial cell differentiation	FOXA2, S100A7, FOXN1, SPRR2G, EHF, SPRR2E, JAG1, SCEL, KDR, RHCG, EREG, SPRR2D, SPRR1B, SPRR2A, VEGFA, SPRR2B, CNFN, SPRR3
Biological Process	response to wounding	TPST1, PPARD, S100A8, FOXA2, TNC, S100A9, GPR68, CDH3, SAA2, CCL20, SAA1, HMOX1, SERPINE1, SERPINA3, VNN1, TFPI2, BLNK, FN1, PLAT, KLK6, KLK8, LYN, CYP1A1, IL1RN, CCL4L1, SAA4, GRHL3, S100A12, PLAUR, NOTCH3, NOTCH2, THBD, EREG, TFPI, SPRR3, ALOX5
Biological Process	angiogenesis	BMP4, S100A7, EDN1, ANPEP, JAG1, THY1, KDR, MAP3K7, VEGFC, EREG, HMOX1, VEGFA, CCBE1, RBPJ, ANGPTL4, CYR61

	Down regulated genes - p < 0.01 - 365	
Category	**Term**	**Genes**
Cytoband	1q21-q22	SPRR2D, SPRR1B, SPRR2A, SPRR2B, SPRR3, SPRR2G, SPRR2E
Cytoband	1q21	MUC1, S100A8, PGLYRP4, S100A7, PGLYRP3, S100A9, ARNT, S100A12, HIST1H4H
Biological Process	ectoderm development	KLK7, PPARD, S100A7, CRABP2, KLK5, FOX
Biological Process	response to wounding	PPARD, S100A8, TNC, S100A9, GPR68, CDH3, CCL20, SAA2, SAA1, HMOX1, SERPINE1, SERPINA3, VNN1, BLNK, PLAT, KLK6, KLK8, LYN, CYP1A1, IL1RN, SAA4, CCL4L1, GRHL3, S100A12, PLAUR, NOTCH3, NOTCH2, THBD, TFPI, SPRR3, ALOX5
Biological Process	epithelial cell differentiation	S100A7, FOXN1, SPRR2G, EHF, SPRR2E, SCEL, RHCG, SPRR2D, SPRR2A, SPRR1B, SPRR2B, CNFN, SPRR3
Biological Process	keratinization	SPRR2D, SPRR1B, SPRR2A, CNFN, SPRR2B, SPRR3, SPRR2G, SPRR2E

	Upregulated - p < 0.01 - 132	
Category	**Term**	**Genes**
Biological Process	angiogenesis	BMP4, VEGFC, EREG, CCBE1, VEGFA, ANPEP, JAG1, RBPJ, KDR, THY1, ANGPTL4
Biological Process	blood vessel morphogenesis	ZFP36L1, BMP4, VEGFC, EREG, CCBE1, VEGFA, ANPEP, JAG1, RBPJ, KDR, THY1, ANGPTL4

D

E

F

G
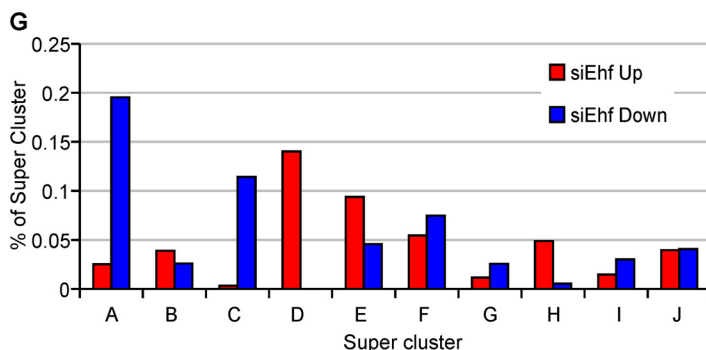
transport and oxidative phosphorylation, and protein translation. The GO analysis also identified categories that correspond to the morphological changes observed in the cornea, such as an increase in epithelial cell differentiation and a decrease in cell adhesion and cell motion. We also discovered that of these aging-regulated genes, a disproportionate number are stroma-enriched. This may relate to the quiescent state of keratocytes (4) as opposed to the constant cell renewal in the epithelium.

We also identified three cornea- and cornea epithelium-enriched genes in the aging data set, *Slurp1*, *1600014C10Rik*, and *Ehf*. SLURP1, which plays an immunomodulatory role in the cornea epithelium, suppressing neutrophil infiltration, is down-regulated in proinflammatory conditions of the cornea (67). The down-regulation of *Slurp1* in aging may suggest decreased immune privilege in aging but also suggests potentially a quicker response to injury. The human ortholog of *1600014C10Rik*, *C19orf12*, encodes a small mitochondrially localized protein that may play a role in lipid homeostasis (92). Mutations in this gene are associated with some cases of neurodegeneration with iron accumulation in the brain (92). In the adult cornea, *1600014C10Rik* is moderately expressed and down-regulated to an unusual extent (-7.41-fold) in aging, suggesting that it may play a role in decreased mitochondrial function in the cornea, potentially leading to increased oxidative stress and increased cellular damage. The *Ehf* gene, which is up-regulated during aging, promotes cornea epithelial differentiation (see below); EHF may contribute to the increased epithelial differentiation in the aging cornea.

Our findings on gene expression during cornea aging support some of the general principles derived by previous meta-analyses of aging data sets (22, 93). First, relatively few genes change in aging compared with development. Second, the changes across different tissues are relatively unique, although functionally similar tissues do show more similarity than functionally distinct tissues. Finally, although there are relatively few specific genes that change across many tissues, there are several pathways that are commonly age-regulated. However, although we did find individual genes belonging to the following categories, we did not find enrichment for immune response-, inflammation-, or cell cycle-related genes, processes shown to be common across numerous aging organs (93). The lack of differential regulation of genes in these specific categories is informative because it highlights ways that the cornea may be distinct from other tissues. In particular, because one of the primary functions of the cornea is to maintain transparency for vision, the regulation of immune response- and inflammation-related genes must be tightly controlled to prevent changes that disrupt vision.

EHF as a Regulator of Epithelial Cell Fate in the Cornea—EHF (Ets homologous factor), a member of the ESE (epithelial specific expression) Ets transcription factor family (94), caught our interest because 1) it is expressed relatively highly in cornea compared with several other epithelial tissues; 2) it is selectively expressed in the epithelium of the cornea; 3) its temporal expression pattern during cornea development correlates highly with the expression of known cornea differentiation genes in supercluster A, including that of *Aldh3a1* and *Krt12*; and 4) its expression increases during aging, correlating with aging-associated differentiation. Previous studies found that EHF expression is enriched in epithelial tissues (95), particularly glandular epithelia, where it binds targets related to late stage differentiation (96). It has been shown to be highly expressed in cornea (97), conjunctiva (53), and prostate endocrine cells (98), although the roles of EHF in these tissues are yet to be described.

Through siRNA knockdown of *EHF* in cornea epithelial cells, we discovered that epithelium-related genes and genes in the epidermal differentiation complex were down-regulated. These data support our hypothesis that EHF is involved in the epithelial differentiation program of the cornea and suggest that it is primarily a transcriptional activator of these genes. We also found that non-epithelial genes were up-regulated and mapped to stromal superclusters, suggesting that EHF is also a repressor of non-epithelial/stromal genes within cornea epithelial cells.

We performed *in vivo* ChIP-seq of separated cornea epithelium and compared it with the siRNA data to identify genes both bound and regulated by EHF, thus further elucidating the role of EHF in the cornea epithelium. Multiple genes involved in immunity-related functions are differentially regulated, such as *CXCL14* (2.65-fold), *SGPP2* (-2.12-fold), and *PLAUR* (-1.38-fold). CXCL14, a chemokine shown to be up-regulated in epidermal cell differentiation (99), may play a role in immune function of differentiated cornea epithelium. However, it is also known to play a role in cell migration and angiogenesis, and its up-regulation after *EHF* knockdown points to a role of EHF in

FIGURE 10. **EHF ChIP-seq, in combination with gene expression data from cornea epithelial cells lacking EHF, indicates that EHF is a regulator of cornea epithelial cell identity.** *A*, mRNA levels of *EHF* in human cornea epithelial cells after siRNA knockdown (si*EHF*) compared with a scrambled control (siCtrl) (*left*) and EHF protein levels in scrambled control and si*EHF* immortalized human cornea epithelial cells (*right*). *B*, overlap between developmental superclusters (Fig. 3) and genes significantly altered after *EHF* knockdown in human cornea epithelia cells. *Exp.*, expected number of differentially regulated genes that should overlap based on random distribution. *Act.*, actual number of differentially regulated genes that overlapped; these *bars* are broken into up-regulated and down-regulated genes after *EHF* knockdown. An enrichment of down-regulated genes is found in superclusters A, C, and G, which are enriched for epithelia expressed genes. In contrast, up-regulated genes are enriched in superclusters B, D, and E, which are enriched for stroma expressed genes. *C*, enrichment of GO terms among all differentially regulated, down-regulated, and up-regulated genes after EHF knockdown. Down-regulated genes are strongly associated with biological functions linked to epithelial identity and function. *D*, overlap of EHF ChIP-seq peaks linked to genes (*blue*; 6075 total) and genes differentially regulated after *EHF* knockdown (*red*). Approximately half of the genes affected by *EHF* knockdown contain a linked EHF ChIP-seq peak. *E*, gene ontology of genes both differentially regulated in the *EHF* siRNA experiments and bound by EHF. These genes are strongly linked to morphogenesis and epithelium development. *F*, the relationship between genes bound and regulated by EHF and the expression levels, arranged as quintiles (*I–V*), of these genes in mouse cornea epithelium. There is a positive correlation between expression level in mouse cornea epithelium and genes that appear to be up-regulated by EHF. In contrast, there is a negative correlation between expression level in mouse cornea epithelium and genes that appear to be repressed by EHF. *G*, membership of EHF bound and regulated genes in the cornea expression superclusters; these genes are divided into up-regulated (*siEHF Up*) and down-regulated (*siEHF Down*) genes after EHF knockdown. The genes that appear to be activated by EHF fall most prominently into superclusters A and C, both of which are linked to epithelial development. In contrast, genes that appear to be repressed by EHF fall most prominently into superclusters D and E, both of which are primarily associated with stromal gene expression.

suppressing this function. SGPP2 is involved in lipid metabolism and may be induced during the inflammatory response (100). The regulation of these genes suggests a role for EHF in regulating the immune response of the differentiated cornea epithelium. The cornea is both highly innervated and populated by antigen-presenting cells (101), and EHF may be involved in regulating signaling to these cells. Other interesting EHF-regulated genes that we identified with the combined ChIP-Seq/siRNA experiment include *CCNA1* (2.24-fold), *FGFR3* (−1.9-fold), and *TCF4* (1.36-fold). FGFR3 plays a role in negative regulation of epithelial proliferation (102) and positive regulation of epithelial cell commitment (103, 104), whereas CCNA1 plays a role in regulation of the cell cycle (104). TCF4 is associated with proliferation in limbal epithelial stem cells and is not expressed in more differentiated cornea epithelial cells (71). Together, our data suggest that EHF modulates epithelial cell fate through repression of proliferation and non-epithelial genes and activation of epithelial differentiation and immunity-related genes.

The discovery of a role for EHF in the cornea epithelium provides an example of the utility of the cornea transcriptome profile. Through the time course data, we gained insights into the potential role of EHF and its target genes, which we verified through ChIP and knockdown studies. Interestingly, we found predicted KLF4 and KLF5 binding sites within a significant portion of the EHF ChIP-seq peaks. Furthermore, we found that ~30% of the genes deregulated after either *Klf4* or *Klf5* gene deletion in the cornea contain EHF peaks in their close proximity. Together, these data suggest the possibility that EHF collaborates with KLF4 and KLF5 to specify cornea epithelial cell identity.

REFERENCES

1. Greiling, T. M., and Clark, J. I. (2008) The transparent lens and cornea in the mouse and zebra fish eye. *Semin. Cell Dev. Biol.* **19,** 94–99
2. Pei, Y. F., and Rhodin, J. A. (1970) The prenatal development of the mouse eye. *Anat. Rec.* **168,** 105–125
3. Hay, E. D. (1980) Development of the vertebrate cornea. *Int. Rev. Cytol.* **63,** 263–322
4. Zieske, J. D. (2004) Corneal development associated with eyelid opening. *Int. J. Dev. Biol.* **48,** 903–911
5. Cavallotti, C., and Cerulli, L. (2010) *Age-related Changes of the Human Eye*, pp. 45–57, Humana Press, New York
6. Fitch, K. L., and Nadakavukaren, M. J. (1986) Age-related changes in the corneal endothelium of the mouse. *Exp. Gerontol.* **21,** 31–35
7. Sevel, D., and Isaacs, R. (1988) A re-evaluation of corneal development. *Trans. Am. Ophthalmol. Soc.* **86,** 178–207
8. Sheldon, H. (1956) An electron microscope study of the epithelium in the normal mature and immature mouse cornea. *J. Biophys. Biochem. Cytol.* **2,** 253–262
9. Wu, F., Lee, S., Schumacher, M., Jun, A., and Chakravarti, S. (2008) Differential gene expression patterns of the developing and adult mouse cornea compared to the lens and tendon. *Exp. Eye Res.* **87,** 214–225
10. Chakravarti, S., Wu, F., Vij, N., Roberts, L., and Joyce, S. (2004) Microarray studies reveal macrophage-like function of stromal keratocytes in the cornea. *Invest. Ophthalmol. Vis. Sci.* **45,** 3475–3484
11. Norman, B., Davis, J., and Piatigorsky, J. (2004) Postnatal gene expression in the normal mouse cornea by SAGE. *Invest. Ophthalmol. Vis. Sci.* **45,** 429–440
12. Gipson, I. K., and Grill, S. M. (1982) A technique for obtaining sheets of intact rabbit corneal epithelium. *Invest. Ophthalmol. Vis. Sci.* **23,** 269–273
13. Yu, Z., Mannik, J., Soto, A., Lin, K. K., and Andersen, B. (2009) The epidermal differentiation-associated Grainyhead gene Get1/Grhl3 also regulates urothelial differentiation. *EMBO J.* **28,** 1890–1903
14. Dudoit, S., Gentleman, R. C., and Quackenbush, J. (2003) Open source software for the analysis of microarray data. *BioTechniques* **Suppl,** 45–51
15. Saeed, A. I., Bhagabati, N. K., Braisted, J. C., Liang, W., Sharov, V., Howe, E. A., Li, J., Thiagarajan, M., White, J. A., and Quackenbush, J. (2006) TM4 microarray software suite. *Methods Enzymol.* **411,** 134–193
16. Kayala, M. A., and Baldi, P. (2012) Cyber-T web server. Differential analysis of high-throughput data. *Nucleic Acids Res.* **40,** W553–W559
17. Baldi, P., and Long, A. D. (2001) A Bayesian framework for the analysis of microarray expression data. Regularized t test and statistical inferences of gene changes. *Bioinformatics* **17,** 509–519
18. Carbon, S., Ireland, A., Mungall, C. J., Shu, S., Marshall, B., and Lewis, S. (2009) AmiGO. Online access to ontology and annotation data. *Bioinformatics* **25,** 288–289
19. Huang, H., Lu, X., Liu, Y., Haaland, P., and Marron, J. S. (2012) R/DWD. Distance-weighted discrimination for classification, visualization and batch adjustment. *Bioinformatics* **28,** 1182–1183
20. Edgar, R., Domrachev, M., and Lash, A. E. (2002) Gene Expression Omnibus. NCBI gene expression and hybridization array data repository. *Nucleic Acids Res.* **30,** 207–210
21. Barrett, T., Troup, D. B., Wilhite, S. E., Ledoux, P., Evangelista, C., Kim, I. F., Tomashevsky, M., Marshall, K. A., Phillippy, K. H., Sherman, P. M., Muertter, R. N., Holko, M., Ayanbule, O., Yefanov, A., and Soboleva, A. (2011) NCBI GEO. Archive for functional genomics data sets. 10 years on. *Nucleic Acids Res.* **39,** D1005–D1010
22. Zahn, J. M., Poosala, S., Owen, A. B., Ingram, D. K., Lustig, A., Carter, A., Weeraratna, A. T., Taub, D. D., Gorospe, M., Mazan-Mamczarz, K., Lakatta, E. G., Boheler, K. R., Xu, X., Mattson, M. P., Falco, G., Ko, M. S., Schlessinger, D., Firman, J., Kummerfeld, S. K., Wood, W. H., 3rd, Zonderman, A. B., Kim, S. K., and Becker, K. G. (2007) AGEMAP. A gene expression database for aging in mice. *PLoS Genet.* **3,** e201
23. Brink, T. C., Demetrius, L., Lehrach, H., and Adjaye, J. (2009) Age-related transcriptional changes in gene expression in different organs of mice support the metabolic stability theory of aging. *Biogerontology* **10,** 549–564
24. Bianchi-Frias, D., Vakar-Lopez, F., Coleman, I. M., Plymate, S. R., Reed, M. J., and Nelson, P. S. (2010) The effects of aging on the molecular and cellular composition of the prostate microenvironment. *PLoS One* **5,** e12501
25. Swindell, W. R., Johnston, A., Sun, L., Xing, X., Fisher, G. J., Bulyk, M. L., Elder, J. T., and Gudjonsson, J. E. (2012) Meta-profiles of gene expression during aging. Limited similarities between mouse and human and an unexpectedly decreased inflammatory signature. *PLoS One* **7,** e33204
26. Misra, V., Lee, H., Singh, A., Huang, K., Thimmulappa, R. K., Mitzner, W., Biswal, S., and Tankersley, C. G. (2007) Global expression profiles from C57BL/6J and DBA/2J mouse lungs to determine aging-related genes. *Physiol. Genomics* **31,** 429–440
27. Someya, S., Yamasoba, T., Prolla, T. A., and Tanokura, M. (2007) Genes encoding mitochondrial respiratory chain components are profoundly down-regulated with aging in the cochlea of DBA/2J mice. *Brain Res.* **1182,** 26–33
28. Rossi, D. J., Bryder, D., Zahn, J. M., Ahlenius, H., Sonu, R., Wagers, A. J., and Weissman, I. L. (2005) Cell intrinsic alterations underlie hematopoietic stem cell aging. *Proc. Natl. Acad. Sci. U.S.A.* **102,** 9194–9199
29. Kohman, R. A., Rodriguez-Zas, S. L., Southey, B. R., Kelley, K. W., Dantzer, R., and Rhodes, J. S. (2011) Voluntary wheel running reverses age-induced changes in hippocampal gene expression. *PLoS One* **6,** e22654
30. Verbitsky, M., Yonan, A. L., Malleret, G., Kandel, E. R., Gilliam, T. C., and Pavlidis, P. (2004) Altered hippocampal transcript profile accompanies an age-related spatial memory deficit in mice. *Learn Mem.* **11,** 253–260

31. Edwards, M. G., Anderson, R. M., Yuan, M., Kendziorski, C. M., Weindruch, R., and Prolla, T. A. (2007) Gene expression profiling of aging reveals activation of a p53-mediated transcriptional program. *BMC Genomics* **8,** 80

32. Oberdoerffer, P., Michan, S., McVay, M., Mostoslavsky, R., Vann, J., Park, S. K., Hartlerode, A., Stegmuller, J., Hafner, A., Loerch, P., Wright, S. M., Mills, K. D., Bonni, A., Yankner, B. A., Scully, R., Prolla, T. A., Alt, F. W., and Sinclair, D. A. (2008) SIRT1 redistribution on chromatin promotes genomic stability but alters gene expression during aging. *Cell* **135,** 907–918

33. Hamatani, T., Falco, G., Carter, M. G., Akutsu, H., Stagg, C. A., Sharov, A. A., Dudekula, D. B., VanBuren, V., and Ko, M. S. (2004) Age-associated alteration of gene expression patterns in mouse oocytes. *Hum. Mol. Genet.* **13,** 2263–2278

34. Beggs, M. L., Nagarajan, R., Taylor-Jones, J. M., Nolen, G., Macnicol, M., and Peterson, C. A. (2004) Alterations in the TGFβ signaling pathway in myogenic progenitors with age. *Aging Cell* **3,** 353–361

35. Ida, H., Boylan, S. A., Weigel, A. L., and Hjelmeland, L. M. (2003) Age-related changes in the transcriptional profile of mouse RPE/choroid. *Physiol. Genomics* **15,** 258–262

36. Lustig, A., Carter, A., Bertak, D., Enika, D., Vandanmagsar, B., Wood, W., Becker, K. G., Weeraratna, A. T., and Taub, D. D. (2009) Transcriptome analysis of murine thymocytes reveals age-associated changes in thymic gene expression. *Int. J. Med. Sci.* **6,** 51–64

37. Huang da, W., Sherman, B. T., and Lempicki, R. A. (2009) Systematic and integrative analysis of large gene lists using DAVID bioinformatics resources. *Nat. Protoc.* **4,** 44–57

38. Huang da, W., Sherman, B. T., and Lempicki, R. A. (2009) Bioinformatics enrichment tools. Paths toward the comprehensive functional analysis of large gene lists. *Nucleic Acids Res.* **37,** 1–13

39. Hopkin, A. S., Gordon, W., Klein, R. H., Espitia, F., Daily, K., Zeller, M., Baldi, P., and Andersen, B. (2012) GRHL3/GET1 and trithorax group members collaborate to activate the epidermal progenitor differentiation program. *PLoS Genet.* **8,** e1002829

40. Schmidt, D., Wilson, M. D., Spyrou, C., Brown, G. D., Hadfield, J., and Odom, D. T. (2009) ChIP-seq. Using high-throughput sequencing to discover protein-DNA interactions. *Methods* **48,** 240–248

41. Langmead, B., Trapnell, C., Pop, M., and Salzberg, S. L. (2009) Ultrafast and memory-efficient alignment of short DNA sequences to the human genome. *Genome Biol.* **10,** R25

42. Zhang, Y., Liu, T., Meyer, C. A., Eeckhoute, J., Johnson, D. S., Bernstein, B. E., Nusbaum, C., Myers, R. M., Brown, M., Li, W., and Liu, X. S. (2008) Model-based analysis of ChIP-Seq (MACS). *Genome Biol.* **9,** R137

43. Blankenberg, D., Von Kuster, G., Coraor, N., Ananda, G., Lazarus, R., Mangan, M., Nekrutenko, A., and Taylor, J. (2010) Galaxy. A web-based genome analysis tool for experimentalists. *Curr. Protoc. Mol. Biol.*, Chapter 19, Unit 19.10.11–21

44. Giardine, B., Riemer, C., Hardison, R. C., Burhans, R., Elnitski, L., Shah, P., Zhang, Y., Blankenberg, D., Albert, I., Taylor, J., Miller, W., Kent, W. J., and Nekrutenko, A. (2005) Galaxy. A platform for interactive large-scale genome analysis. *Genome Res.* **15,** 1451–1455

45. Goecks, J., Nekrutenko, A., and Taylor, J. (2010) Galaxy. A comprehensive approach for supporting accessible, reproducible, and transparent computational research in the life sciences. *Genome Biol.* **11,** R86

46. Liu, T., Ortiz, J. A., Taing, L., Meyer, C. A., Lee, B., Zhang, Y., Shin, H., Wong, S. S., Ma, J., Lei, Y., Pape, U. J., Poidinger, M., Chen, Y., Yeung, K., Brown, M., Turpaz, Y., and Liu, X. S. (2011) Cistrome. An integrative platform for transcriptional regulation studies. *Genome Biol.* **12,** R83

47. Bailey, T. L., Boden, M., Buske, F. A., Frith, M., Grant, C. E., Clementi, L., Ren, J., Li, W. W., and Noble, W. S. (2009) MEME SUITE. Tools for motif discovery and searching. *Nucleic Acids Res.* **37,** W202–W208

48. Sax, C. M., Salamon, C., Kays, W. T., Guo, J., Yu, F. X., Cuthbertson, R. A., and Piatigorsky, J. (1996) Transketolase is a major protein in the mouse cornea. *J. Biol. Chem.* **271,** 33568–33574

49. Liu, C. Y., Shiraishi, A., Kao, C. W., Converse, R. L., Funderburgh, J. L., Corpuz, L. M., Conrad, G. W., and Kao, W. W. (1998) The cloning of mouse keratocan cDNA and genomic DNA and the characterization of its expression during eye development. *J. Biol. Chem.* **273,** 22584–22588

50. Yoshida, N., Yoshida, S., Araie, M., Handa, H., and Nabeshima, Y. (2000) Ets family transcription factor ESE-1 is expressed in corneal epithelial cells and is involved in their differentiation. *Mech. Dev.* **97,** 27–34

51. Nakamura, H., Chiambaretta, F., Sugar, J., Sapin, V., and Yue, B. Y. (2004) Developmentally regulated expression of KLF6 in the mouse cornea and lens. *Invest. Ophthalmol. Vis. Sci.* **45,** 4327–4332

52. Tanifuji-Terai, N., Terai, K., Hayashi, Y., Chikama, T., and Kao, W. W. (2006) Expression of keratin 12 and maturation of corneal epithelium during development and postnatal growth. *Invest. Ophthalmol. Vis. Sci.* **47,** 545–551

53. Davis, J., Davis, D., Norman, B., and Piatigorsky, J. (2008) Gene expression of the mouse corneal crystallin Aldh3a1. Activation by Pax6, Oct1, and p300. *Invest. Ophthalmol. Vis. Sci.* **49,** 1814–1826

54. Nakamura, T., Ohtsuka, T., Sekiyama, E., Cooper, L. J., Kokubu, H., Fullwood, N. J., Barrandon, Y., Kageyama, R., and Kinoshita, S. (2008) Hes1 regulates corneal development and the function of corneal epithelial stem/progenitor cells. *Stem Cells* **26,** 1265–1274

55. Kao, W. W., Liu, C. Y., Converse, R. L., Shiraishi, A., Kao, C. W., Ishizaki, M., Doetschman, T., and Duffy, J. (1996) Keratin 12-deficient mice have fragile corneal epithelia. *Invest. Ophthalmol. Vis. Sci.* **37,** 2572–2584

56. Estey, T., Piatigorsky, J., Lassen, N., and Vasiliou, V. (2007) ALDH3A1. A corneal crystallin with diverse functions. *Exp. Eye Res.* **84,** 3–12

57. Adachi, W., Okubo, K., and Kinoshita, S. (2000) Human uroplakin Ib in ocular surface epithelium. *Invest. Ophthalmol. Vis. Sci.* **41,** 2900–2905

58. Swamynathan, S. K., Katz, J. P., Kaestner, K. H., Ashery-Padan, R., Crawford, M. A., and Piatigorsky, J. (2007) Conditional deletion of the mouse *Klf4* gene results in corneal epithelial fragility, stromal edema, and loss of conjunctival goblet cells. *Mol. Cell Biol.* **27,** 182–194

59. Kenchegowda, D., Harvey, S. A., Swamynathan, S., Lathrop, K. L., and Swamynathan, S. K. (2012) Critical role of Klf5 in regulating gene expression during post-eyelid opening maturation of mouse corneas. *PLoS One* **7,** e44771

60. Verkman, A. S., Ruiz-Ederra, J., and Levin, M. H. (2008) Functions of aquaporins in the eye. *Prog. Retin. Eye Res.* **27,** 420–433

61. Stepp, M. A. (2006) Corneal integrins and their functions. *Exp. Eye Res.* **83,** 3–15

62. Liu, Y., Peng, X., Tan, J., Darling, D. S., Kaplan, H. J., and Dean, D. C. (2008) Zeb1 mutant mice as a model of posterior corneal dystrophy. *Invest. Ophthalmol. Vis. Sci.* **49,** 1843–1849

63. Kitamura, K., Miura, H., Miyagawa-Tomita, S., Yanazawa, M., Katoh-Fukui, Y., Suzuki, R., Ohuchi, H., Suehiro, A., Motegi, Y., Nakahara, Y., Kondo, S., and Yokoyama, M. (1999) Mouse Pitx2 deficiency leads to anomalies of the ventral body wall, heart, extra- and periocular mesoderm and right pulmonary isomerism. *Development* **126,** 5749–5758

64. Weaving, L., Mihelec, M., Storen, R., Sosic, D., Grigg, J. R., Tam, P. P., and Jamieson, R. V. (2010) Twist2. Role in corneal stromal keratocyte proliferation and corneal thickness. *Invest. Ophthalmol. Vis. Sci.* **51,** 5561–5570

65. Grässel, S., Sicot, F. X., Gotta, S., and Chu, M. L. (1999) Mouse fibulin-2 gene. Complete exon-intron organization and promoter characterization. *Eur. J. Biochem.* **263,** 471–477

66. Trackman, P. C. (2005) Diverse biological functions of extracellular collagen processing enzymes. *J. Cell Biochem.* **96,** 927–937

67. Swamynathan, S., Buela, K. A., Kinchington, P., Lathrop, K. L., Misawa, H., Hendricks, R. L., and Swamynathan, S. K. (2012) Klf4 regulates the expression of Slurp1, which functions as an immunomodulatory peptide in the mouse cornea. *Invest. Ophthalmol. Vis. Sci.* **53,** 8433–8446

68. Faragher, R. G., Mulholland, B., Tuft, S. J., Sandeman, S., and Khaw, P. T. (1997) Aging and the cornea. *Br. J. Ophthalmol.* **81,** 814–817

69. Kaeberlein, M., and Kennedy, B. K. (2011) Hot topics in aging research. Protein translation and TOR signaling, 2010. *Aging Cell* **10,** 185–190

70. Berk, R. S., Katar, M., Dong, Z., and Day, D. E. (2001) Plasminogen activators and inhibitors in the corneas of mice infected with *Pseudomonas aeruginosa*. *Invest. Ophthalmol. Vis. Sci.* **42,** 1561–1567

71. Lu, R., Qu, Y., Ge, J., Zhang, L., Su, Z., Pflugfelder, S. C., and Li, D. Q. (2012) Transcription factor TCF4 maintains the properties of human corneal epithelial stem cells. *Stem Cells* **30,** 753–761

72. Swamynathan, S. K., Davis, J., and Piatigorsky, J. (2008) Identification of

candidate Klf4 target genes reveals the molecular basis of the diverse regulatory roles of Klf4 in the mouse cornea. *Invest. Ophthalmol. Vis. Sci.* **49,** 3360–3370

73. Wei, G. H., Badis, G., Berger, M. F., Kivioja, T., Palin, K., Enge, M., Bonke, M., Jolma, A., Varjosalo, M., Gehrke, A. R., Yan, J., Talukder, S., Turunen, M., Taipale, M., Stunnenberg, H. G., Ukkonen, E., Hughes, T. R., Bulyk, M. L., and Taipale, J. (2010) Genome-wide analysis of ETS-family DNA-binding *in vitro* and *in vivo*. *EMBO J.* **29,** 2147–2160

74. Samstein, R. M., Arvey, A., Josefowicz, S. Z., Peng, X., Reynolds, A., Sandstrom, R., Neph, S., Sabo, P., Kim, J. M., Liao, W., Li, M. O., Leslie, C., Stamatoyannopoulos, J. A., and Rudensky, A. Y. (2012) Foxp3 exploits a pre-existent enhancer landscape for regulatory T cell lineage specification. *Cell* **151,** 153–166

75. Farnham, P. J. (2009) Insights from genomic profiling of transcription factors. *Nat. Rev. Genet.* **10,** 605–616

76. Marenholz, I., Zirra, M., Fischer, D. F., Backendorf, C., Ziegler, A., and Mischke, D. (2001) Identification of human epidermal differentiation complex (EDC)-encoded genes by subtractive hybridization of entire YACs to a gridded keratinocyte cDNA library. *Genome Res.* **11,** 341–355

77. Cabral, A., Voskamp, P., Cleton-Jansen, A. M., South, A., Nizetic, D., and Backendorf, C. (2001) Structural organization and regulation of the small proline-rich family of cornified envelope precursors suggest a role in adaptive barrier function. *J. Biol. Chem.* **276,** 19231–19237

78. Marsden, M. D., and Fournier, R. E. (2005) Organization and expression of the human serpin gene cluster at 14q32.1. *Front. Biosci.* **10,** 1768–1778

79. Chu, W. M. (2013) Tumor necrosis factor. *Cancer Lett.* **328,** 222–225

80. Uhlar, C. M., and Whitehead, A. S. (1999) Serum amyloid A, the major vertebrate acute-phase reactant. *Eur. J. Biochem.* **265,** 501–523

81. Gallagher, G., Dickensheets, H., Eskdale, J., Izotova, L. S., Mirochnitchenko, O. V., Peat, J. D., Vazquez, N., Pestka, S., Donnelly, R. P., and Kotenko, S. V. (2000) Cloning, expression and initial characterization of interleukin-19 (IL-19), a novel homologue of human interleukin-10 (IL-10). *Genes Immun.* **1,** 442–450

82. Pei, Y. F., and Rhodin, J. A. (1971) Electron microscopic study of the development of the mouse corneal epithelium. *Invest. Ophthalmol.* **10,** 811–825

83. Song, J., Lee, Y. G., Houston, J., Petroll, W. M., Chakravarti, S., Cavanagh, H. D., and Jester, J. V. (2003) Neonatal corneal stromal development in the normal and lumican-deficient mouse. *Invest. Ophthalmol. Vis. Sci.* **44,** 548–557

84. Hanlon, S. D., Patel, N. B., and Burns, A. R. (2011) Assessment of postnatal corneal development in the C57BL/6 mouse using spectral domain optical coherence tomography and microwave-assisted histology. *Exp. Eye Res.* **93,** 363–370

85. Tomasek, J. J., Hay, E. D., and Fujiwara, K. (1982) Collagen modulates cell shape and cytoskeleton of embryonic corneal and fibroma fibroblasts. Distribution of actin, α-actinin, and myosin. *Dev. Biol.* **92,** 107–122

86. Higbee, R. G., and Hazlett, L. D. (1983) Actin filament localization and distribution in the young adult mouse cornea. A correlative immunofluorescent and cytochemical study. *Exp. Eye Res.* **36,** 171–180

87. Jester, J. V., Barry, P. A., Lind, G. J., Petroll, W. M., Garana, R., and Cavanagh, H. D. (1994) Corneal keratocytes. *In situ* and *in vitro* organization of cytoskeletal contractile proteins. *Invest. Ophthalmol. Vis. Sci.* **35,** 730–743

88. Cai, L., Fritz, D., Stefanovic, L., and Stefanovic, B. (2010) Nonmuscle myosin-dependent synthesis of type I collagen. *J. Mol. Biol.* **401,** 564–578

89. Allocco, D. J., Kohane, I. S., and Butte, A. J. (2004) Quantifying the relationship between co-expression, co-regulation and gene function. *BMC Bioinformatics* **5,** 18

90. Yu, H., Luscombe, N. M., Qian, J., and Gerstein, M. (2003) Genomic analysis of gene expression relationships in transcriptional regulatory networks. *Trends Genet.* **19,** 422–427

91. Franco, H. L., Casasnovas, J., Rodríguez-Medina, J. R., and Cadilla, C. L. (2011) Redundant or separate entities? Roles of Twist1 and Twist2 as molecular switches during gene transcription. *Nucleic Acids Res.* **39,** 1177–1186

92. Hartig, M. B., Iuso, A., Haack, T., Kmiec, T., Jurkiewicz, E., Heim, K., Roeber, S., Tarabin, V., Dusi, S., Krajewska-Walasek, M., Jozwiak, S., Hempel, M., Winkelmann, J., Elstner, M., Oexle, K., Klopstock, T., Mueller-Felber, W., Gasser, T., Trenkwalder, C., Tiranti, V., Kretzschmar, H., Schmitz, G., Strom, T. M., Meitinger, T., and Prokisch, H. (2011) Absence of an orphan mitochondrial protein, c19orf12, causes a distinct clinical subtype of neurodegeneration with brain iron accumulation. *Am. J. Hum. Genet.* **89,** 543–550

93. de Magalhães, J. P., Curado, J., and Church, G. M. (2009) Meta-analysis of age-related gene expression profiles identifies common signatures of aging. *Bioinformatics* **25,** 875–881

94. Bochert, M. A., Kleinbaum, L. A., Sun, L. Y., and Burton, F. H. (1998) Molecular cloning and expression of Ehf, a new member of the ets transcription factor/oncoprotein gene family. *Biochem. Biophys. Res. Commun.* **246,** 176–181

95. Tugores, A., Le, J., Sorokina, I., Snijders, A. J., Duyao, M., Reddy, P. S., Carlee, L., Ronshaugen, M., Mushegian, A., Watanaskul, T., Chu, S., Buckler, A., Emtage, S., and McCormick, M. K. (2001) The epithelium-specific ETS protein EHF/ESE-3 is a context-dependent transcriptional repressor downstream of MAPK signaling cascades. *J. Biol. Chem.* **276,** 20397–20406

96. Kas, K., Finger, E., Grall, F., Gu, X., Akbarali, Y., Boltax, J., Weiss, A., Oettgen, P., Kapeller, R., and Libermann, T. A. (2000) ESE-3, a novel member of an epithelium-specific ets transcription factor subfamily, demonstrates different target gene specificity from ESE-1. *J. Biol. Chem.* **275,** 2986–2998

97. Gupta, D., Harvey, S. A., Kaminski, N., and Swamynathan, S. K. (2011) Mouse conjunctival forniceal gene expression during postnatal development and its regulation by Kruppel-like factor 4. *Invest. Ophthalmol. Vis. Sci.* **52,** 4951–4962

98. Kobberup, S., Nyeng, P., Juhl, K., Hutton, J., and Jensen, J. (2007) ETS-family genes in pancreatic development. *Dev. Dyn.* **236,** 3100–3110

99. Ikoma, T., Ozawa, S., Suzuki, K., Kondo, T., Maehata, Y., Lee, M. C., Hata, R., and Kubota, E. (2012) Calcium-calmodulin signaling induced by epithelial cell differentiation upregulates BRAK/CXCL14 expression via the binding of SP1 to the BRAK promoter region. *Biochem. Biophys. Res. Commun.* **420,** 217–222

100. Mechtcheriakova, D., Wlachos, A., Sobanov, J., Kopp, T., Reuschel, R., Bornancin, F., Cai, R., Zemann, B., Urtz, N., Stingl, G., Zlabinger, G., Woisetschläger, M., Baumruker, T., and Billich, A. (2007) Sphingosine 1-phosphate phosphatase 2 is induced during inflammatory responses. *Cell. Signal.* **19,** 748–760

101. Mastropasqua, L., Nubile, M., Lanzini, M., Carpineto, P., Ciancaglini, M., Pannellini, T., Di Nicola, M., and Dua, H. S. (2006) Epithelial dendritic cell distribution in normal and inflamed human cornea. *In vivo* confocal microscopy study. *Am. J. Ophthalmol.* **142,** 736–744

102. Arnaud-Dabernat, S., Kritzik, M., Kayali, A. G., Zhang, Y. Q., Liu, G., Ungles, C., and Sarvetnick, N. (2007) FGFR3 is a negative regulator of the expansion of pancreatic epithelial cells. *Diabetes* **56,** 96–106

103. Govindarajan, V., and Overbeek, P. A. (2001) Secreted FGFR3, but not FGFR1, inhibits lens fiber differentiation. *Development* **128,** 1617–1627

104. Gopinathan, L., Ratnacaram, C. K., and Kaldis, P. (2011) Established and novel Cdk/cyclin complexes regulating the cell cycle and development. *Results Probl. Cell Differ.* **53,** 365–389

105. Nakamura, H., Ueda, J., Sugar, J., and Yue, B. Y. (2005) Developmentally regulated expression of Sp1 in the mouse cornea. *Invest. Ophthalmol. Vis. Sci.* **46,** 4092–4096